MECHANISTIC MODELING OF LONGITUDINAL SHAPE CHANGES: EQUATIONS OF MOTION AND INVERSE PROBLEMS

DAI-NI HSIEH[†], SYLVAIN ARGUILLÈRE[‡], NICOLAS CHARON[†], AND
LAURENT YOUNES[†]

[†]*Department of Applied Mathematics and Statistics, Johns Hopkins University*

[‡]*Laboratoire Paul Painlevé, Université de Lille*

ABSTRACT. This paper examines a longitudinal shape evolution model in which a 3D volume progresses through a family of elastic equilibria in response to the time-derivative of an internal force, or yank, with an additional regularization to ensure diffeomorphic transformations. We consider two different models of yank and address the long time existence and uniqueness of solutions for the equations of motion in both models. In addition, we derive sufficient conditions for the existence of an optimal yank that best describes the change from an observed initial volume to an observed volume at a later time. The main motivation for this work is the understanding of processes such as growth and atrophy in anatomical structures, where the yank could be roughly interpreted as a metabolic event triggering morphological changes. We provide preliminary results on simple examples to illustrate, under this model, the retrievability of some attributes of such events.

1. INTRODUCTION

We analyze in this paper a shape evolution paradigm introduced in [18] in which a volume progresses along a family of regularized elastic equilibria controlled by the gradient of a time-dependent potential, this gradient being interpreted as the time-derivative of an internal force that we will refer to as "yank", following, e.g., [20]. A primary motivation of our work is the modeling of shape changes in anatomical structures, where the driving potential may be loosely interpreted as a result of metabolic events, for example, caused by a disease in the structure. Potential applications of this framework include biological growth models [13, 22, 2, 30, 16] or longitudinal studies in computational anatomy, and in particular, slow changes in the brain resulting from neuro-degenerative diseases [7, 8, 5, 26, 19, 21, 29, 15, 1, 37, 31, 35]. Such processes of pathogenesis are not well understood today. Thus we introduce a general framework under which more advanced models can be developed. In our experiments, we make very simple assumptions on the initiation and propagation of the potential. We then illustrate the possibility of inferring the causes of the shape changes only from geometric observations.

The relationship between shape and yank in our model can be represented as a control system in which the velocity field at a given time is obtained as the solution of a linear

---

equation that depends on both. We will provide conditions ensuring that this control system has a unique solution over an arbitrary time interval before formulating and studying the inverse problem of estimating an optimal yank based only on observed initial and final shapes. We will consider two situations in this context. In the first model, we will assume that the yank is unspecified at all times. We will then estimate the yank so that it minimizes a cost accumulating over time, resulting in an optimal control problem. In the second one, the assumption will be that the potential specifying the yank is fully characterized by its initial value and follows the shape transformation through basic advection. In this latter case, we will attempt to solve the inverse problem of determining this initial value (specified by a few parameters) based on partial information on the deformation, namely the boundary of the transformed volume.

The overall paradigm defining the dynamical system is the same as that described in [18], where we assume that, at time t, an infinitesimal force $\delta F(t)$ is applied to a volume $M(t)$ in a zero-stress state, resulting in a new equilibrium at time $t + \delta t$, denoted by $M(t + \delta t)$, where δt is small, therefore assuming that times needed to reach new equilibria are negligible compared to the time frame within which the whole process is considered. (Such an assumption of *evolving reference configuration* is typical in morphoelastic growth models [32, 13, 17].) The new configuration $M(t + \delta t)$ is obtained by displacing each point x in $M(t)$ by a small vector δx, which is obtained by solving a linear equation $\mathcal{L}(t)\delta x = \delta F(t)$, where $\mathcal{L}$ typically depends on M. Dividing by δt, introducing the velocity $v = \delta x/\delta t$ and the yank $j = \delta F/\delta t$, we are led to consider shape evolution processes in which M is advected by the vector field v as the solution of $\mathcal{L}(t)v = j$. The existence of solutions of such a process is stated in Theorems 1 and 2 under some assumptions on the operator $\mathcal{L}$ (which are satisfied, in particular, by properly regularized elastic operators) and on the yank j. Existence of solutions to the inverse problem of estimating j from the initial and final shapes are provided in the same theorems.

The paper is organized as follows. Notation and a general description of our framework are provided in section 2. Our main theorems are stated in section 3 and proved in section 6. Section 4 provides specific examples to which our theorems apply. Section 5 presents experimental results. We conclude with a discussion in section 7 and provide implementation details in Appendix A.

2. Formulation of problems

2.1. **Notation.** For an integer $s \geq 0$, we let $C_0^s(\mathbb{R}^3, \mathbb{R}^3)$ denote the space of s-times continuously differentiable vector fields v such that the kth derivative $D^k v$ tends to 0 at infinity for every $k \leq s$. The space $C_0^s(\mathbb{R}^3, \mathbb{R}^3)$ is a Banach space equipped with the norm $\|v\|_{s,\infty} = \sum_{k=0}^{s} \max_{x \in \mathbb{R}^3} |D^k v(x)|$, where $|\cdot|$ denotes the operator norm of a multilinear map on a product of finite-dimensional vector spaces equipped with the Euclidean norm. If $s = 0$, we will write the customary $\|v\|_\infty$ instead of $\|v\|_{0,\infty}$.

Let $id : \mathbb{R}^3 \to \mathbb{R}^3$ be the identity map, i.e., $id(x) = x$. We denote by $Diff_{id}^s(\mathbb{R}^3)$ the set of C^s diffeomorphisms on $\mathbb{R}^3$ that tend to identity at infinity. Thus every element $\varphi \in Diff_{id}^s(\mathbb{R}^3)$ can be written as $\varphi = id + v$, where $v \in C_0^s(\mathbb{R}^3, \mathbb{R}^3)$. The affine Banach space $id + C_0^s(\mathbb{R}^3, \mathbb{R}^3)$ is equipped with the induced metric $d(\varphi, \psi) = \|\varphi - \psi\|_{s,\infty}$, which makes $Diff_{id}^s(\mathbb{R}^3) \subset id + C_0^s(\mathbb{R}^3, \mathbb{R}^3)$ an open subset.

We will denote by $\mathscr{L}(B, \widetilde{B})$ the vector space of bounded linear operators from a Banach space B to another Banach space $\widetilde{B}$. Weak convergence of sequences (x_n) in B will be

denoted by $x_n \rightharpoonup x$. Denoting the topological dual of B by B^*, we will use the notation $(\mu \,|\, v)$ rather than $\mu(v)$ to denote the evaluation of $\mu \in B^*$ at $v \in B$. We say a linear operator $A \in \mathscr{L}(B, B^*)$ is symmetric if the corresponding bilinear form $(v, w) \mapsto (Av \,|\, w)$ is symmetric. The subspace of symmetric linear operators will be denoted by $\mathscr{L}_{\mathrm{sym}}(B, B^*)$.

For a generic function $f : [0, T] \times \mathbb{R}^3 \to \mathbb{R}^3$, we will use the notation $f(t) : \mathbb{R}^3 \to \mathbb{R}^3$ defined by $f(t)(x) = f(t, x)$. We will use C to denote a generic constant and C_a to show a generic constant depending on a. The value of such constants may change from equation to equation.

Throughout this paper, V is a separable Hilbert space of vector fields on $\mathbb{R}^3$ continuously embedded in $C_0^2(\mathbb{R}^3, \mathbb{R}^3)$, which is denoted by $V \hookrightarrow C_0^2(\mathbb{R}^3, \mathbb{R}^3)$, with inner product $\langle \cdot, \cdot \rangle_V$ and norm $\| \cdot \|_V$. Since $V \hookrightarrow C_0^2(\mathbb{R}^3, \mathbb{R}^3)$, there exists a constant c_V such that $\|v\|_{2,\infty} \leq c_V \|v\|_V$. The duality map $L_V : V \to V^*$ is given by

$$(L_V \, v \,|\, w) = \langle v, \, w \rangle_V$$

and provides an isometry from V onto V^*. We denote the inverse of L_V by $K_V \in \mathscr{L}(V^*, V)$, which, because of the embedding assumption, is a kernel operator [4]. Note that

$$\|v\|_V^2 = (L_V \, v \,|\, v) = (K_V^{-1} v \,|\, v).$$

As an example, the space V can be the reproducing kernel Hilbert space (RKHS) associated with a Matérn kernel of some order r, and some width σ, which, in three dimensions, implies that V is a Sobolev space H^{r+2}. For the specific value $r = 3$, which we will use in our experiments, the kernel operator (when applied to a vector measure $\mu \in V^*$) takes the form

$$(K_V \, \mu)(x) = \int_{\mathbb{R}^3} \kappa(|x - y|/\sigma) \, d\mu(y)$$

with $\kappa(t) = (1 + t + 2t^2/15 + t^3/15)e^{-t}$.

If B is a Banach space and $p \geq 1$, $L^p([0, T], B)$ denotes the space of Bochner integrable functions $f : [0, T] \to B$ such that $\int_0^T \|f(t)\|_B^p \, dt < \infty$. Recall that a function $f : [0, T] \to B$ is Bochner integrable if: (i) it is the almost-everywhere limit of a sequence of measurable functions that take a finite number of values (also called simple functions) and (ii) satisfies $\int_0^T \|f(t)\|_B \, dt < \infty$.

2.2. **Control systems and inverse problems.** We now describe the dynamics we consider in this paper, which gradually deform shapes through elastic equilibria. We assume a mapping $A : Diff_{id}^1(\mathbb{R}^3) \to \mathscr{L}_{\mathrm{sym}}(V, V^*)$ defined by $\varphi \mapsto A_\varphi$. Given a time-dependent mapping $j : [0, T] \to V^*$, we model the deformation trajectory of a compact subset $M_0 \subset \mathbb{R}^3$ as $t \mapsto \varphi_j(t, M_0)$, where $\varphi_j \in C([0, T], Diff_{id}^1(\mathbb{R}^3))$ is a solution to the system

$$\begin{cases} \partial_t \varphi(t, x) = v(t, \varphi(t, x)), \ \varphi(0, x) = x, \\ v(t) = \underset{v' \in V}{\arg\min} \ \frac{\omega}{2} \, \|v'\|_V^2 + \frac{1}{2} \, (A_{\varphi(t)} \, v' \,|\, v') - (j(t) \,|\, v') \end{cases} \tag{1}$$

and $\omega > 0$ is a fixed regularization parameter. The first equation in this system will be seen as an ordinary differential equation in $Diff_{id}^1(\mathbb{R}^3)$. We can interpret the squared norm $\frac{\omega}{2} \, \|v'\|_V^2$ as a regularization term that is introduced to ensure that $v(t)$ and (as we will see in our results) $\varphi(t) - id$ are both in $C_0^2(\mathbb{R}^2, \mathbb{R}^2)$. This term will also ensure that $\varphi(t)$ is a diffeomorphism at all times (similar regularizations were used in works such as [6, 33, 34]). The operator $A_{\varphi(t)}$, as we shall detail later, may be for instance an elastic operator in

which case the second term $\frac{1}{2}\left(A_{\varphi(t)}\,v'\,|\,v'\right)$ represents the linear elastic energy associated to the deformation while $j(t)$ represents a yank inducing the motion of the material. In this context, the second equation in system (1) essentially states that the deformation vector field at each time is governed by an infinitesimal version of the principle of virtual work [24, Theorem 1.6, Chapter 5] with regularization. As a result, the shape $\varphi_j(t, M_0)$ is deformed from a stress-free state to an equilibrium at all time in this dynamical system, as described earlier in the introduction. We postpone specific examples of elastic operators and yank until section 4, after presenting sufficient conditions ensuring existence of solutions of our inverse problems in section 3, where we treat A_φ and j as general operators.

We let $\mathscr{M}$ denote a class of compact subsets of $\mathbb{R}^3$ that represents our "shape space" and assume that it is stable by the action of diffeomorphisms, i.e., $\varphi(\mathscr{M}) \subset \mathscr{M}$ for all $\varphi \in Diff_{id}^1(\mathbb{R}^3)$. A specific description of $\mathscr{M}$ is problem dependent (see Remark 3). Given two elements $M_0, M_{\text{targ}} \in \mathscr{M}$, providing the observed initial shape and final shape, or target, we aim to find j within a given class such that the deformed M_0 in response to j at time T, i.e., $\varphi_j(T, M_0)$, is close to M_{targ} in some sense. Closeness will be measured according to a discrepancy function $\rho : \mathscr{M} \times \mathscr{M} \to [0, +\infty)$ that compares compact sets (see examples in Remark 3). We will focus on the following two frameworks regarding the time-dependent yank j:

(1) Free yank model. In system (1), one can interpret j as a control that drives the evolution of the state φ through the vector field v_φ. Let $\mathcal{X}_{V^*, T}^p = L^p([0, T], V^*)$. We will consider the optimal control problem

$$\min_{j \in \mathcal{X}_{V^*, T}^2} \int_0^T (j(t)\,|\,v(t))\,dt + \rho(\varphi(T, M_0), M_{\text{targ}}) \tag{2}$$

subject to system (1). We will give sufficient conditions guaranteeing the existence of solutions of this problem in Theorem 1.

(2) Parametric yank model. The yank is modeled as a function of a transformation φ and of a finite-dimensional parameter θ belonging to a compact set $\Theta \subset \mathbb{R}^m$. In this case, the finite-dimensional optimization problem of interest is

$$\min_{\theta \in \Theta}\ \rho(\varphi(T, M_0), M_{\text{targ}}) \tag{3}$$

subject to (1) with $j(t) = j(\varphi(t), \theta)$, namely,

$$\begin{cases} \partial_t\,\varphi(t, x) = v(t, \varphi(t, x)),\ \ \varphi(0, x) = x, \\[2mm] v(t) = \arg\min_{v' \in V} \dfrac{\omega}{2}\,\|v'\|_V^2 + \dfrac{1}{2}\left(A_{\varphi(t)}\,v'\,|\,v'\right) - (j(\varphi(t), \theta)\,|\,v'). \end{cases} \tag{4}$$

Examples of such yanks are provided in section 4. We give sufficient conditions for this optimization problem to have a solution in Theorem 2.

3. Main results

Given a compact subset $\Omega \subset \mathbb{R}^3$, we define the seminorm

$$\|v\|_{s,\infty}^\Omega = \sum_{k=1}^s \max_{x \in \Omega} |D^k v(x)|$$

on $C^s(\mathbb{R}^3, \mathbb{R}^3)$. We require a regularity assumption on the discrepancy function ρ appearing in the objective functionals (2) and (3).

Definition 1. *We say that a discrepancy function $\rho : \mathscr{M} \times \mathscr{M} \to [0, +\infty)$ is continuous on $\mathscr{M}$ with respect to $\| \cdot \|_{s,\infty}$ if for all compact sets $M, M' \in \mathscr{M}$ and all sequences $(\varphi_n)_{n=1}^{\infty} \subset Diff_{id}^s(\mathbb{R}^3)$ such that $\|\varphi_n - \varphi\|_{s,\infty}^M \to 0$ for some $\varphi \in Diff_{id}^s(\mathbb{R}^3)$, one has*

$$\rho(\varphi_n(M), M') \to \rho(\varphi(M), M').$$

Theorem 1 (Free yank model). *Let $A : Diff_{id}^1(\mathbb{R}^3) \to \mathscr{L}_{\mathrm{sym}}(V, V^*)$ be a mapping defined by $\varphi \mapsto A_\varphi$. Assume that $(A_\varphi v \,|\, v) \geq 0$ for all $\varphi \in Diff_{id}^1(\mathbb{R}^3)$ and $v \in V$. Let the two compact sets $M_0, M_{\mathrm{targ}} \in \mathscr{M}$ be given. Then the following results hold.*

(i) *Suppose that $\varphi \mapsto A_\varphi$ is locally Lipschitz (for the $\| \cdot \|_{1,\infty}$ distance). Then, given $j \in \mathcal{X}_{V^*,T}^1$, the system*

$$\begin{cases} \partial_t \varphi(t,x) = v(t, \varphi(t,x)), \ \varphi(0,x) = x, \\ v(t) = \underset{v' \in V}{\arg\min} \ \dfrac{\omega}{2} \|v'\|_V^2 + \dfrac{1}{2} \left(A_{\varphi(t)} v' \,|\, v'\right) - (j(t) \,|\, v') \end{cases} . \tag{1}$$

has a unique solution $\varphi \in C([0,T], Diff_{id}^2(\mathbb{R}^3))$.

(ii) *Suppose that, for each $\gamma > 0$, the mapping $\varphi \mapsto A_\varphi$ is Lipschitz with respect to the seminorm $\| \cdot \|_{1,\infty}^{M_0}$ on*

$$\mathfrak{S}_\gamma = \{\varphi \in Diff_{id}^1(\mathbb{R}^3) : \|\varphi - id\|_{1,\infty} \leq \gamma \text{ and } \|\varphi^{-1} - id\|_{1,\infty} \leq \gamma\}.$$

In addition, assume that the discrepancy function ρ is continuous on $\mathscr{M}$ with respect to $\| \cdot \|_{1,\infty}$. Then there exists a minimizer of the optimal control problem

$$\min_{j \in \mathcal{X}_{V^*,T}^2} \int_0^T (j(t) \,|\, v(t)) \, dt + \rho(\varphi(T, M_0), M_{\mathrm{targ}})$$

where v and φ satisfy (1).

Before stating our next theorem, we remind the reader that a collection of functions is said to be equi-Lipschitz if they are all Lipschitz and there exists a common Lipschitz constant that applies to all functions in the collection.

Theorem 2 (Parametric yank model). *Let $A : Diff_{id}^1(\mathbb{R}^3) \to \mathscr{L}_{\mathrm{sym}}(V, V^*)$ be a mapping defined by $\varphi \mapsto A_\varphi$. Assume that $(A_\varphi v \,|\, v) \geq 0$ for all $\varphi \in Diff_{id}^1(\mathbb{R}^3)$ and $v \in V$. Moreover, let $\Theta \subset \mathbb{R}^m$ be a compact set and let $j : Diff_{id}^1(\mathbb{R}^3) \times \Theta \to V^*$. Finally, let two compact sets $M_0, M_{\mathrm{targ}} \in \mathscr{M}$ be given. Then the following results hold.*

(i) *Suppose that $\varphi \mapsto A_\varphi$ is locally Lipschitz and that $\varphi \mapsto j(\varphi, \theta)$ is locally Lipschitz (in both cases for $\| \cdot \|_{1,\infty}$ distance) and bounded in norm. Given $\theta \in \Theta$, the system*

$$\begin{cases} \partial_t \varphi(t,x) = v(t, \varphi(t,x)), \ \varphi(0,x) = x, \\ v(t) = \underset{v' \in V}{\arg\min} \ \dfrac{\omega}{2} \|v'\|_V^2 + \dfrac{1}{2} \left(A_{\varphi(t)} v' \,|\, v'\right) - (j(\varphi(t), \theta) \,|\, v') \end{cases} . \tag{4}$$

has a unique solution $\varphi \in C([0,T], Diff_{id}^2(\mathbb{R}^3))$.

(ii) *Suppose that:*

- *For each $\gamma > 0$, the mapping $\varphi \mapsto A_\varphi$ is Lipschitz and the family of mappings $\{j(\cdot, \theta) : \theta \in \Theta\}$ is equi-Lipschitz, both with respect to the seminorm $\|\cdot\|_{1,\infty}^{M_0}$, on the set*

$$\mathfrak{S}_\gamma = \{\varphi \in \mathit{Diff}_{id}^1(\mathbb{R}^3) : \|\varphi - id\|_{1,\infty} \leq \gamma \text{ and } \|\varphi^{-1} - id\|_{1,\infty} \leq \gamma\}.$$

- *For all $\varphi \in \mathit{Diff}_{id}^1(\mathbb{R}^3)$, $j(\varphi, \cdot)$ is continuous in the sense that*

$$\theta_n \to \theta \quad implies \quad j(\varphi, \theta_n) \rightharpoonup j(\varphi, \theta).$$

- *There exists a constant J_Θ such that*

$$\|j(\varphi, \theta)\|_{V^*} \leq J_\Theta \quad for \ all \ \varphi \in \mathit{Diff}_{id}^1(\mathbb{R}^3) \ and \ \theta \in \Theta.$$

- *The discrepancy function ρ is continuous on $\mathscr{M}$ with respect to $\|\cdot\|_{1,\infty}$.*

Then there exists a minimizer for the finite-dimensional optimization problem

$$\min_{\theta \in \Theta} \ \rho(\varphi(T, M_0), M_{\mathrm{targ}})$$

where φ satisfies (4).

We will prove these two theorems in section 6. Both control systems can be considered as ordinary differential equations with values in the affine Banach space $id + C_0^1(\mathbb{R}^d, \mathbb{R}^d)$. Most of the effort in proving the long-time existence and uniqueness of solutions, part (i) of the theorems, will rely on controlling the vector field $v(t)$ by the input, j in the first case and θ in the second case. A key step for this is provided by Lemma 2(iii), which exploits the regularization term $\frac{\omega}{2} \|v'\|_V^2$. After this key step, we can carry out a proof using the Banach fixed point theorem and the Picard iteration in the space $C([0, T], \mathit{Diff}_{id}^1(\mathbb{R}^3))$. Due to the regularity of the vector field, Lemma 3 will show that the obtained unique solution is actually in $C([0, T], \mathit{Diff}_{id}^2(\mathbb{R}^3))$. For part (ii) of the theorems, we will use the direct method of calculus of variations to prove the existence of minimizers. Denoting the objective function by f, the two key steps of the direct method are proving that a minimizing sequence is bounded and that f is weakly sequentially lower semicontinuous. The choice of the objective function affects the first step (see Remark 2). To accomplish the second step, we need to show $f(j) \leq \liminf_{n \to \infty} f(j_n)$ for any sequence $j_n \rightharpoonup j$. We prove this by going through an intermediate step:

$$j_n \rightharpoonup j \ \Rightarrow \ \|\varphi_{j_n}(t) - \varphi_j(t)\|_{1,\infty}^{M_0} \to 0 \ \Rightarrow \ f(j) \leq \liminf_{n \to \infty} f(j_n),$$

where φ_{j_n} and φ_j are solutions given j_n and j respectively. The seminorm $\|\cdot\|_{1,\infty}^{M_0}$ is adopted to resolve a difficulty in this intermediate step: although $j_n \rightharpoonup j$ implies $\varphi_{j_n}(t, x) \to \varphi_j(t, x)$ pointwise, we do note have the uniform convergence. Fortunately, the convergence in the seminorm given by the Arzelà–Ascoli theorem suffices.

Remark 1. We stated our theorems in dimension three because it corresponds to most interesting situations in practice, but our proofs apply without change to any dimension (and we are providing some experimental illustrations in dimension two).

Remark 2. The choice we made for the control cost $(j \,|\, v)$ in Theorem 1 is one among a large spectrum of costs for which the conclusions of the theorem are valid. We took this specific example for simplicity and also because it provided the best results in our experiments among some other options we tried. Other possible examples could be $\|j\|_{V^*}^2$, or $\|j\|_{L^2}^2$, for

which our proofs can easily be modified (actually, simplified), with details being left to the reader.

Remark 3. In the experiments presented in this paper, we will use discrepancy functions based on the varifold pseudo-metrics introduced in [11] between certain surfaces associated with the two volumes (e.g., their boundaries). In this case, $\mathscr{M}$ is the set of all compact subsets $M \subset \mathbb{R}^3$ whose boundary ∂M is a rectifiable surface (we refer to [28] for the precise definition and properties of rectifiable sets). Then, given M and M' in $\mathscr{M}$, for S and S' two rectifiable surfaces extracted from M and M' (such as for instance the boundaries of the volumes or some corresponding internal layers) the discrepancy function takes the following form:

$$\rho(M, M') = \nu(S, S) - 2\nu(S, S') + \nu(S', S')$$

with

$$\nu(S, S') = \int_S \int_{S'} \chi\left(\frac{|x - x'|}{\tau}\right) (n(x)^\top n'(x'))^2 \, d\sigma(x) \, d\sigma'(x')$$

where σ and σ' are volume measures on S and S', n and n' are unit normal vector fields of S and S' and χ is some radial kernel function, scaled by a scalar $\tau > 0$, which in our experiments is taken to be the Cauchy kernel

$$\chi(t) = (1 + t^2)^{-2}.$$

It can be then shown, cf., [10, Proposition 6], that such discrepancy functions are continuous on $\mathscr{M}$ with respect to $\| \cdot \|_{1,\infty}$, in the sense of Definition 1.

As a side note, one could alternatively select ρ as the volume of the symmetric difference between the two sets, i.e., $\rho(M, M') = \text{vol}(M \triangle M')$ which is continuous on compact sets with respect to $\| \cdot \|_{0,\infty}$ and thus also with respect to $\| \cdot \|_{1,\infty}$, thereby satisfying the assumption of the above theorems. In this case, the shape space $\mathscr{M}$ is composed of all compact subsets of $\mathbb{R}^3$.

Remark 4. A model based on principles that are similar to ours has been introduced and studied in [9] in order to model tissue growth. In [9], the second equation in system (1) is replaced by the minimization of an isotropic linear elastic energy under the constraint that $\text{div } v = g(u)$, where g is a fixed function and u is the concentration of morphogen, a growth-induced chemical produced by cells. The concentration of morphogen is controlled by the density of cells via a linear elliptic equation, and the density of cells is advected under the motion. While we consider here more general elasticity models, inducing additional complications in the analysis because these elastic properties must also be advected along the flow, the main difference between the two models results from the regularization $\frac{\omega}{2} \|v'\|_V^2$ added in (1). It is this term that guarantees the regularity of the vector field v (see Lemma 1) and allows us to prove long-time existence of solutions, while [9] only obtains local existence results. Such a property is necessary to formulate optimal control problems, which form the second focus of our paper, and could not be addressed in [9].

4. Examples of elastic operators and yank

In this section, we provide examples of elastic operators and yank that satisfy the conditions in Theorems 1 and 2. Denote the space of symmetric bilinear forms on the space

of 3-by-3 symmetric matrices by $\Sigma_2(\mathrm{Sym}_3(\mathbb{R}), \mathrm{Sym}_3(\mathbb{R}))$. Given $\varphi \in Diff_{id}^1(\mathbb{R}^3)$, an elastic operator $A_\varphi \in \mathscr{L}_{\mathrm{sym}}(V, V^*)$ takes the following form

$$(A_\varphi u \,|\, v) = \int_{\varphi(M_0)} E_\varphi(\varepsilon_u, \varepsilon_v) \, dx = \int_{\varphi(M_0)} (E_\varphi(x))(\varepsilon_u(x), \varepsilon_v(x)) \, dx, \qquad (5)$$

where $E_\varphi : \varphi(M_0) \to \Sigma_2(\mathrm{Sym}_3(\mathbb{R}), \mathrm{Sym}_3(\mathbb{R}))$ is a stiffness tensor after the shape is deformed by φ, and ε_u and ε_v are linear strain tensors defined by

$$\varepsilon_u = \frac{1}{2}\left(Du + Du^\top\right) \quad \text{and} \quad \varepsilon_v = \frac{1}{2}\left(Dv + Dv^\top\right).$$

We recall the basic assumption in our model that the deformed configuration becomes a new reference for the next infinitesimal shape changes (with material properties advected by the flow). This is reflected in equation (5).

A simple example, assuming that the elastic property of an isotropic elastic material is unaffected by deformation, or persistent, is provided by $E_\varphi(\varepsilon_u, \varepsilon_v) = \lambda \operatorname{tr}(\varepsilon_u) \operatorname{tr}(\varepsilon_v) + 2\mu \operatorname{tr}(\varepsilon_u^\top \varepsilon_v)$, where λ and μ are the Lamé parameters. More generally, the following proposition proved in section 6 provides a sufficient condition on the mapping $\varphi \mapsto E_\varphi$ ensuring that the corresponding A_φ satisfies the conditions of Theorems 1 and 2.

Proposition 1. *Suppose that $E_\varphi(x)$ is positive definite for all $\varphi \in Diff_{id}^1(\mathbb{R}^3)$ and $x \in \varphi(M_0)$. Moreover, suppose that, for each $\gamma > 0$, there exists $\alpha_\gamma > 0$ such that*

$$\int_{M_0} |E_\varphi \circ \varphi - E_\psi \circ \psi| \, dx \le \alpha_\gamma \, \|\varphi - \psi\|_{1,\infty}^{M_0} \quad \text{for all } \varphi, \psi \in \mathfrak{S}_\gamma, \qquad (6)$$

where

$$\mathfrak{S}_\gamma = \{\varphi \in Diff_{id}^1(\mathbb{R}^3) : \|\varphi - id\|_{1,\infty} \le \gamma \text{ and } \|\varphi^{-1} - id\|_{1,\infty} \le \gamma.\}$$

Then, for A_φ defined as in (5), the mapping $\varphi \mapsto A_\varphi$ satisfies the conditions of Theorems 1 and 2.

Example 1. According to Proposition 1, the simplest example of the elastic operator is when the stiffness tensor E_φ is constant and positive definite since the left-hand side of (6) is zero. Thus our example of persistent isotropic elastic material, i.e., $E_\varphi(\varepsilon_u, \varepsilon_v) = \lambda \operatorname{tr}(\varepsilon_u) \operatorname{tr}(\varepsilon_v) + 2\mu \operatorname{tr}(\varepsilon_u^\top \varepsilon_v)$, is a valid choice. More generally, suppose that $\Lambda : M_0 \to \Sigma_2(\mathrm{Sym}_3(\mathbb{R}), \mathrm{Sym}_3(\mathbb{R}))$ and that $\Lambda(x)$ is positive definite for all $x \in M_0$, then $E_\varphi := \Lambda \circ \varphi^{-1}$ also satisfies the conditions in Proposition 1. Note that this form of E_φ preserves the elastic properties of the material from x to $\varphi(x)$.

Example 2. Even more generally, let $F_\varphi : \varphi(M_0) \to GL(3, \mathbb{R})$ be a deformation-dependent frame field, where $GL(3, \mathbb{R})$ denotes the general linear group. We consider stiffness tensors of the form $\widetilde{E}_\varphi(\varepsilon_u, \varepsilon_v) := (\Lambda \circ \varphi^{-1})(F_\varphi^\top \varepsilon_u F_\varphi, F_\varphi^\top \varepsilon_v F_\varphi)$, where Λ is the same as in Example 1.

The following proposition, whose proof is elementary and left to the reader, provides sufficient conditions on F ensuring that $\widetilde{E}$ satisfies the conditions in Proposition 1. Note that in this case, the elastic properties at $\varphi(x)$ are modified from the ones at x through a change of the frame coordinates $F_\varphi(\varphi(x))$.

Proposition 2. *Suppose that E satisfies the conditions in Proposition 1. Let $F_\varphi : \mathbb{R}^3 \to GL(3, \mathbb{R})$ be essentially bounded for each $\varphi \in Diff_{id}^1(\mathbb{R}^3)$. If there exists $\beta_\gamma > 0$ such that*

$$\|F_\varphi \circ \varphi - F_\psi \circ \psi\|_\infty \le \beta_\gamma \, \|\varphi - \psi\|_{1,\infty}^{M_0} \quad \text{for all } \varphi, \psi \in \mathfrak{S}_\gamma,$$

then $\widetilde{E}$ defined by $\widetilde{E}_\varphi(\varepsilon_u, \varepsilon_v) = E_\varphi(F_\varphi^\top \varepsilon_u F_\varphi, F_\varphi^\top \varepsilon_v F_\varphi)$ also satisfies the conditions in Proposition 1.

Let w_1, w_2, and w_3 be linearly independent vector fields on M_0. Examples of frame fields F_φ that satisfy the previous assumptions include

$$F_\varphi = \left[\ \frac{D\varphi\, w_1}{|D\varphi\, w_1|}, \quad \frac{D\varphi\, w_2}{|D\varphi\, w_2|}, \quad \frac{D\varphi\, w_3}{|D\varphi\, w_3|} \ \right] \circ \varphi^{-1}$$

and

$$F_\varphi = \left[\ \frac{D\varphi\, w_1}{|D\varphi\, w_1|}, \quad \frac{(D\varphi\, w_1 \times D\varphi\, w_2) \times D\varphi\, w_1}{|(D\varphi\, w_1 \times D\varphi\, w_2) \times D\varphi\, w_1|}, \quad \frac{D\varphi\, w_3}{|D\varphi\, w_3|} \ \right] \circ \varphi^{-1}. \tag{7}$$

Note that the first two vectors of the latter F_φ are orthonormal for all deformation φ.

Example 3. An elastic operator inspired by the laminar organization of the cerebral cortex using the frame field (7) was introduced in [18]; we describe it here for completeness. Suppose that a compact subset $M_0 \subset \mathbb{R}^3$ has two surfaces $\mathcal{M}_{\text{bottom}}$ and $\mathcal{M}_{\text{top}}$ as bottom and top layers. Moreover, suppose that we are given a diffeomorphism $\Phi : [0,1] \times \mathcal{M}_{\text{bottom}} \to M_0$ such that $\Phi(0, \mathcal{M}_{\text{bottom}}) = \mathcal{M}_{\text{bottom}}$ and $\Phi(1, \mathcal{M}_{\text{bottom}}) = \mathcal{M}_{\text{top}}$. Note that $\Phi(\nu, \mathcal{M}_{\text{bottom}}) =: \mathcal{M}_\nu$ is a surface for each $\nu \in [0,1]$. We refer to Φ as a layered structure of M_0. Such a structure induces a transversal vector field $S := \partial_\nu \Phi$ (Figure 1). Let T_1 and T_2 be linearly independent vector fields on M_0 such that $T_1|_{\mathcal{M}_\nu}$ and $T_2|_{\mathcal{M}_\nu}$ are tangent to $\mathcal{M}_\nu$. Then, T_1, T_2, and S are linearly independent vector fields on M_0. If we let $w_1 = T_1$, $w_2 = T_2$, and $w_3 = S$ in (7) and define

$$\begin{aligned} \bar{\Lambda}(\varepsilon, \varepsilon) &= \lambda_{\text{tan}}(\varepsilon_{11} + \varepsilon_{22})^2 + \mu_{\text{tan}}(\varepsilon_{11}^2 + \varepsilon_{22}^2 + 2\varepsilon_{12}^2) \\ &\quad + \mu_{\text{tsv}}\, \varepsilon_{33}^2 + \mu_{\text{ang}}(2\varepsilon_{13}^2 + 2\varepsilon_{23}^2), \end{aligned} \tag{8}$$

where ε_{ij} denotes the ijth element of $\varepsilon \in \text{Sym}_3(\mathbb{R})$ and λ_{tan}, μ_{tan}, μ_{tsv}, and μ_{ang} are constants, then the corresponding elastic operator

$$(A_\varphi u \,|\, v) = \int_{\varphi(M_0)} \bar{\Lambda}(F_\varphi^\top \varepsilon_u F_\varphi, F_\varphi^\top \varepsilon_v F_\varphi)\, dx \tag{9}$$

is well-defined [18] and a valid choice by Example 1 and Proposition 2. Note that the layered structure on a deformed shape $\varphi(M_0)$ becomes $(\nu, x) \mapsto \varphi \circ \Phi(\nu, \varphi^{-1}(x))$. The elastic material corresponding to this elastic operator has the property that it is isotropic along the directions tangent to the layers. Figures 2b and 2c illustrate deformations $\varphi_j(T, M_0)$ according to system (1) under different elastic parameters μ_{tan} and μ_{tsv} when we apply the same yank j to a layered shape M_0 (Figure 2a).
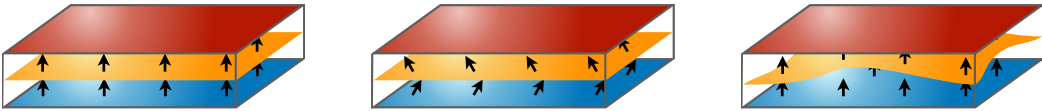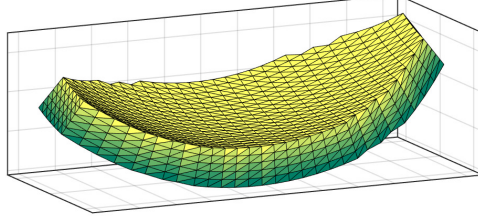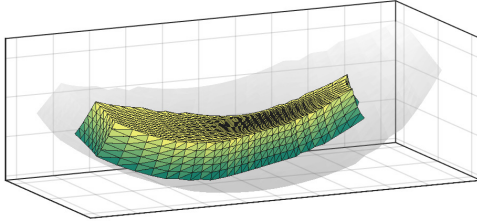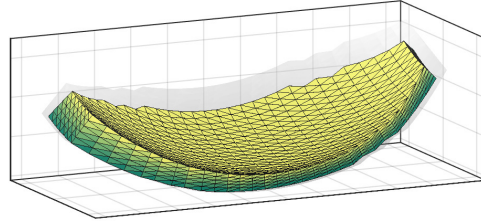

FIGURE 1. Different layered structures of the same rectangular region. Shown in the figures are top layer, one middle layer, bottom layer, and the transversal vector field.

(A) A simulated layered shape.

(B) Tangential deformation.

(C) Transversal deformation.

FIGURE 2. Responses to the same yank under different layered elastic parameters. In (b), $\mu_{\text{tan}} = 0.02\,\mu_{\text{tsv}}$. In (c), $\mu_{\text{tsv}} = 0.02\,\mu_{\text{tan}}$.

Example 4. Now we provide an example of yank which has a density as the gradient of a transported potential. Let $\Theta \subset \mathbb{R}^m$ be a compact set and let $g : \Theta \to L^\infty(\mathbb{R}^3, \mathbb{R})$ defined by $\theta \mapsto g_\theta$. We interpret g_θ as a parametrized potential. We assume that there exists $G_\Theta > 0$ such that $\|g_\theta\|_\infty \le G_\Theta$ for all $\theta \in \Theta$ and $g_{\theta_n}(x) \to g_\theta(x)$ for all $x \in \mathbb{R}^3$ when $\theta_n \to \theta$. For technical reasons, let Ω be a fixed bounded subset of $\mathbb{R}^3$ and let $\chi : \mathbb{R}^3 \to [0,1]$ be a C^∞ cutoff function of compact support such that $\chi_{|\Omega} \equiv 1$. Under this setting, the yank $j(\varphi, \theta)$ defined by

$$(j(\varphi, \theta) \mid v) = - \int_{\varphi(M_0)} \chi\, g_\theta \circ \varphi^{-1} \operatorname{div}(v)\, dx$$

satisfies the conditions in Theorem 2(ii). Note that if $\varphi(M_0) \subset \Omega$ and g_θ is differentiable with support in the interior of M_0, then $(j(\varphi, \theta) \mid v) = \int_{\varphi(M_0)} \nabla(g_\theta \circ \varphi^{-1})^\top v\, dx$. In this case, it follows that $j(\varphi, \theta) = \nabla(g_\theta \circ \varphi^{-1})\, \mathbb{1}_{\varphi(M_0)}\, dx$, which motivates the above formulation.

We check that the conditions on j in Theorem 2(ii) are satisfied. Since

$$|(j(\varphi, \theta) \mid v)| \le \|g_\theta\|_\infty \|v\|_{1,\infty} \|\chi\|_{L^1} \le G_\Theta\, c_V \|v\|_V\, \|\chi\|_{L^1},$$

we see that $j(\varphi, \theta) \in V^*$ for all $\varphi \in Diff^1_{id}(\mathbb{R}^3)$ and $\theta \in \Theta$, and $\|j(\varphi, \theta)\|_{V^*} \le G_\Theta\, c_V \|\chi\|_{L^1} =: J_\Theta$. For a convergent sequence $\theta_n \to \theta$ in Θ, the assumption $g_{\theta_n}(x) \to g_\theta(x)$ for all $x \in \mathbb{R}^3$ and the dominated convergence theorem imply $(j(\varphi, \theta_n) \mid v) \to (j(\varphi, \theta) \mid v)$ for all $\varphi \in Diff^1_{id}(\mathbb{R}^3)$ and $v \in V$. It remains to check that $\{j(\cdot, \theta) : |\theta| \in \Theta\}$ is equi-Lipschitz with respect to the seminorm $\|\cdot\|_{1,\infty}^{M_0}$ on $\mathfrak{S}_\gamma$. Note that $A \mapsto \det A$ is a polynomial of degree 3 in

elements of $A \in \mathbb{R}^{3 \times 3}$. By the mean value theorem, there exists a constant $C > 0$ such that

$$| \det A - \det B | \leq C \left(|A| + |B| \right)^2 |A - B| \tag{10}$$

for all $A, B \in \mathbb{R}^{3 \times 3}$. It follows that, for all $\varphi, \psi \in \mathfrak{S}_\gamma$,

$$
\begin{aligned}
&|(j(\varphi, \theta) \,|\, v) - (j(\psi, \theta) \,|\, v)| \\
&\leq \int_{M_0} \Big| g_\theta \, (\chi \circ \varphi) \, (\mathrm{div}(v) \circ \varphi) \, |\det D\varphi| - g_\theta \, (\chi \circ \psi) \, (\mathrm{div}(v) \circ \psi) \, |\det D\psi| \Big| \, dx \\
&\leq \|g_\theta\|_\infty \Big(\|\nabla \chi\|_\infty \|v\|_{1,\infty} \|\det D\varphi\|_\infty + \|v\|_{2,\infty} \|\det D\varphi\|_\infty \\
&\qquad\qquad + \|v\|_{1,\infty} \, C \, (\|D\varphi\|_\infty + \|D\psi\|_\infty)^2 \Big) \|\varphi - \psi\|_{1,\infty}^{M_0} \, \mathrm{vol}(M_0) \\
&\leq G_\Theta \, C_\gamma \, \|v\|_V \, \|\varphi - \psi\|_{1,\infty}^{M_0},
\end{aligned}
$$

where we have made a change of variables to obtain the first inequality, split the integrand into several terms, then used (10) in the second inequality, and the assumptions $\|g_\theta\|_\infty \leq G_\Theta$ and $\varphi, \psi \in \mathfrak{S}_\gamma$ in the last inequality.

5. Experiments

We performed experiments on simulated and real data. We used 2D simulated data to compare retrieved solutions with known solutions. In all experiments, we assume that shapes have a layered structure described in Example 3 and illustrated in Figure 1. The discrepancy function $\rho(\cdot, \cdot)$ is defined based on the varifold pseudo-metrics of [11] (cf., also Remark 3), and is used to register certain layers of M_0 and M_{targ}. In addition, to prevent applied forces to only induce rigid motions on the generated shapes, our simulations penalize the motion of the bottom layer. This is achieved by adding a penalty to the operator A_φ, replacing the second equation in (1) by

$$v = \underset{v' \in V}{\arg\min} \ \frac{\omega}{2} \|v'\|_V^2 + \frac{1}{2} \left(A_\varphi \, v' \,|\, v' \right) - (j \,|\, v') + \frac{\beta}{2} \int_{\varphi(\mathcal{M}_{\mathrm{bottom}})} (v'^\top n)^2 \, d\sigma, \tag{11}$$

where n is a unit normal vector field to $\varphi(\mathcal{M}_{\mathrm{bottom}})$. Note that we can define

$$(\widetilde{A}_\varphi \, u \,|\, w) = (A_\varphi \, u \,|\, w) + \beta \int_{\varphi(\mathcal{M}_{\mathrm{bottom}})} (u^\top n)(w^\top n) \, d\sigma$$

and apply our results to $\widetilde{A}$. Indeed, the added term satisfies the assumption of Theorems 1 and 2 (this will be justified in section 6 at the end of the proof of Proposition 1).

All computations are implemented in CUDA and run on a computer equipped with GPU NVIDIA GeForce RTX 2080 Ti.

5.1. **2D simulations.** We take V to be the RKHS associated to a Matérn kernel of order 3 with width $\sigma = 0.2$ in our 2D simulations (see subsection 2.1). For the varifold pseudo-metric, we use a Cauchy kernel with width 0.3 for the spatial kernel and a Binet kernel for the Grassmannian kernel (i.e., ρ is as described in Remark 3 with $\tau = 0.3$). We fix the end time $T = 1$.

(A) Template.

(B) Deformed template.

Time 0

Time 0.3

Time 0.6

Time 0.9
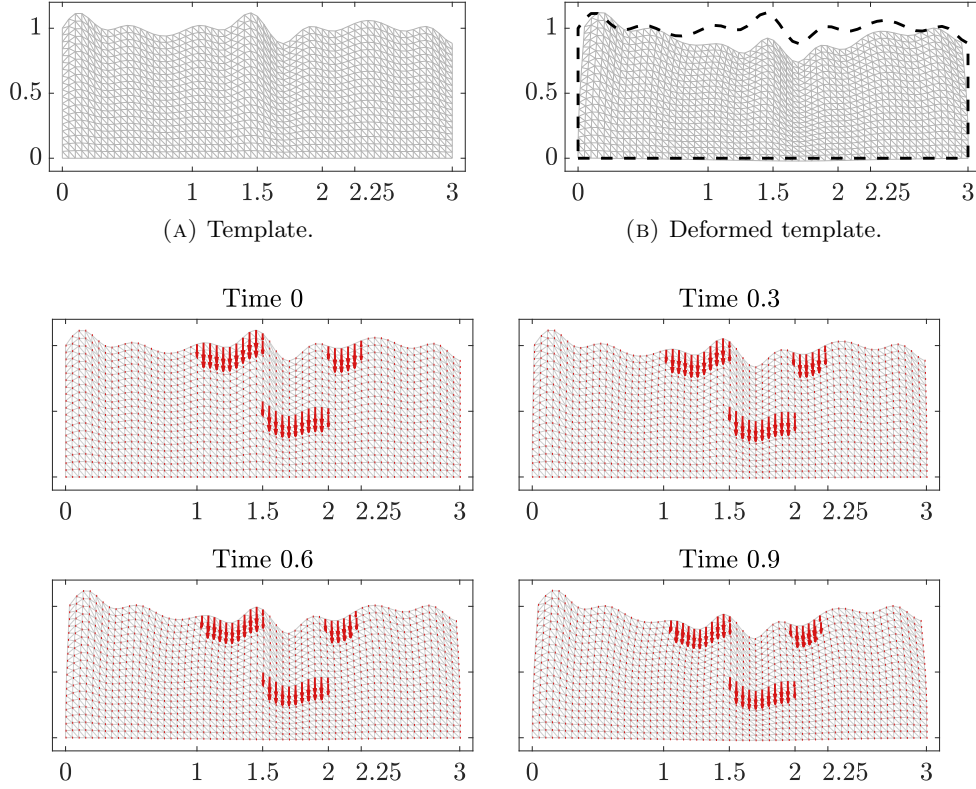
(C) Time-dependent yank used to generate the deformed template in (b) (vectors scaled by 20).

FIGURE 3. Simulated data for the free yank problem.

5.1.1. *Free yank problem.* Figure 3a shows a simulated layered shape with the layered structure $\Phi : [0, 1] \times [0, 3] \to \mathbb{R}^2$ given by

$$\Phi(\nu, x) = \frac{1}{20} \nu \left(20 + \sin(6x) + \frac{1}{2} \sin(10x) + \sin(14x) + \frac{3}{10} \sin(18x) \right).$$

Denote the discretized triangles by $\{\mathcal{T}_k\}_{k=1}^K$. We approximate $j \in V^*$ by a simple function $j = \sum_{k=1}^K j_k \operatorname{area}(\mathcal{T}_k) \mathbb{1}_{\mathcal{T}_k}$, where $\mathbb{1}_{\mathcal{T}_k}$ is the indicator function on $\mathcal{T}_k$. For the purpose of illustration, we generated a deformed shape (Figure 3b) using a yank which is supported in three spatial regions, two on the top layer and one on the middle layer (Figure 3c). The vectors j_k are mapped on the vertices for visualization. Note that the support of the yank is simply advected by the deformation. We used the persistent isotropic elastic operator in this case, that is, $E_\varphi(\varepsilon_u, \varepsilon_v) = \lambda \operatorname{tr}(\varepsilon_u) \operatorname{tr}(\varepsilon_v) + 2\mu \operatorname{tr}(\varepsilon_u^\top \varepsilon_v)$, with $\lambda = 0$ and $\mu = 0.5$. Since we assume that the deformed shape is isotropic at all time, here the layered structure is actually irrelevant to the definition of the elastic operator. Using layers extracted from the deformed shape as targets, we then searched a minimizer of our free yank problem using limited-memory BFGS.

We first consider registering top and bottom layers from "template" (M_0) to "target" (M_{targ}), depicted in Figures 4a and 4b. Assuming the correct elastic model parameters λ and μ are used, the registration and retrieved yank are shown in Figures 4c and 4d. We observe from Figure 4d that large magnitude of the retrieved yank mainly occurs on top and bottom layers. Although the horizontal position of the true yank in the interval $[1, 2.25]$ is captured quite accurately, no yank is found in the middle layer due to the lack of information regarding the internal deformation in the discrepancy cost ρ.

(A) Template.

(B) Simulated target.
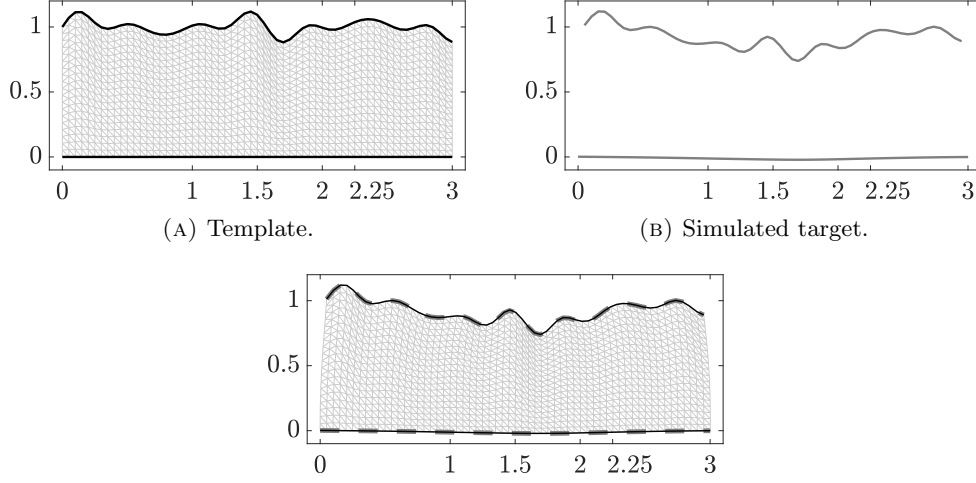
(C) Registration result. The black lines indicate the deformed top and bottom layers of the template; the dashed gray lines indicate the ones of the target.
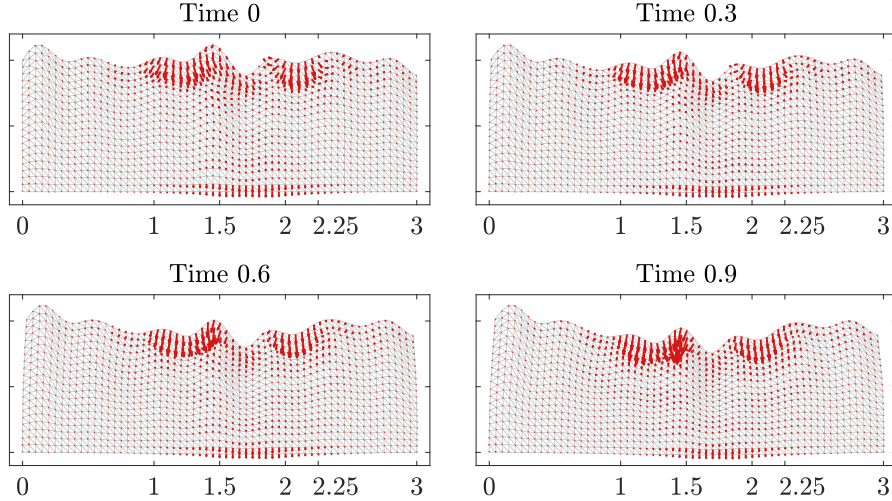
(D) Retrieved time-dependent yank (vectors scaled by 20).

FIGURE 4. Result of the free yank problem registering top and bottom layers.

In comparison, Figure 5 shows the estimated registration and yank when the deformation of of all layers is observed (up to tangential motion along the layers) and taken into account in the matching by adding discrepancy terms for each of these layers. We see that in this case the three spatial regions of support of the true yank can be located. However, observing the internal layer structure of the target is not typical in applications where usually only the external boundary of the considered volumes can be acquired or segmented.

If one does not want to assume that too much information, such as internal displacements, is available from observed data, it becomes necessary to impose more constraints on the yank itself, by assuming that prior information is known on its structure. This motivates our second model using a parametric yank.

5.1.2. *Parametric yank problem.* To mimic the laminar organization of cortical volumes [12, 3], we simulated a layered shape for this experiment. Figure 6a shows our simulated shape whose middle layer is the graph of $x \mapsto 0.25 \cos(2.5(x - 0.1)) + 0.6$. Other layers are generated through normal displacement starting from the middle layer with a step size 0.05. We use a parametric yank of the form of Example 4, that is,

$$(j(\varphi, \theta) \,|\, v) = - \int_{\varphi(M_0)} \chi \; g_\theta \circ \varphi^{-1} \operatorname{div}(v) \, dx.$$

The potential g_θ we used is a C^1 compactly supported function

$$g_{(c,h)}(x; r) = \begin{cases} h \left(\dfrac{|x - c|^2}{r^2} - 1 \right)^2 & \text{if } |x - c| \leq r \\ 0 & \text{otherwise} \end{cases} . \tag{12}$$

Note that the parameter $\theta = (c, h)$ is composed of the center $c = (c_x, c_y) \in \mathbb{R}^2$ and the height $h \in \mathbb{R}$. We assume that the radius r is known. Figure 6b shows the potential with $c = (1.5, 0.5)$, $h = 2$, and $r = 0.25$. Given $\theta = (c, h)$, we then computed the solution φ_θ to the system (4) under the layered elastic operator (equation (8)) with $\lambda_{\text{tan}} = 0$ and $\mu_{\text{tan}} = \mu_{\text{tsv}} = \mu_{\text{ang}} = 1$. The deformation $\varphi_\theta(1, M_0)$ is shown in Figure 6c, and the yank $j(\varphi_\theta(t), \theta)$ is shown in Figure 6d. The top and bottom layers of $\varphi_\theta(1, M_0)$ were extracted as the target for our finite-dimensional optimization problem. Using a BFGS optimization method with multiple starting points sampled by a Latin hypercube design, we can retrieve $(c_x, c_y, h) = (1.5, 0.5, 2)$ within an absolute error 10^{-4}.

We now examine the robustness of our method when r or the elastic parameters that are used in the inverse problem differ from those used to generate the target. In Figure 7, we plot the computed minimizer $\theta^* = (c_x^*, c_y^*, h^*)$ when we fix a different r. While the retrieved height h^* is inversely proportional to the radius r with a fitted relationship $h^* = \mathcal{O}(r^{-2.37})$, the retrieved center (c_x^*, c_y^*) remains close to the true one $(1.5, 0.5)$. We remark that the relationship $h^* = \mathcal{O}(r^{-p})$ was also observed in other simulated shapes, but with a different $p > 0$. The retrieved center is also quite stable when we vary the elastic parameters as we can see from Figure 8, except for very small μ_{tan} or μ_{tsv}.

5.2. **3D real data.** We now propose an experiment using 3D data derived from the BIO-CARD dataset [25], which is a longitudinal study of Alzheimer's disease. More precisely, the template and target shown in Figure 9 were obtained by computing shape averages [23] of scans of the entorhinal cortex of subjects diagnosed with mild cognitive impairment in the cohort, using scans at the beginning of the study for the template, and after ten years of study for the target (the study is still ongoing with new scans being acquired). Participants

(A) Template.

(B) Simulated target.
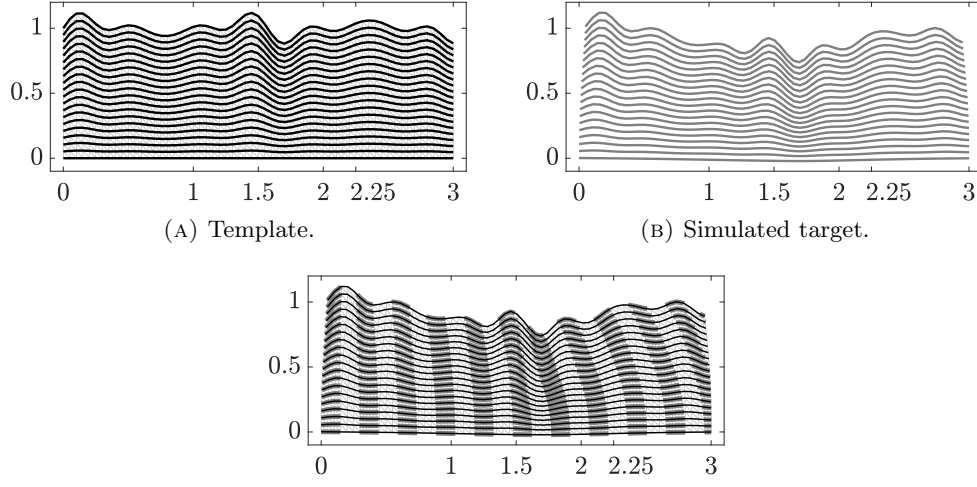
(C) Registration result. The black lines indicate the deformed layers of the template; the dashed gray lines indicate the ones of the target.
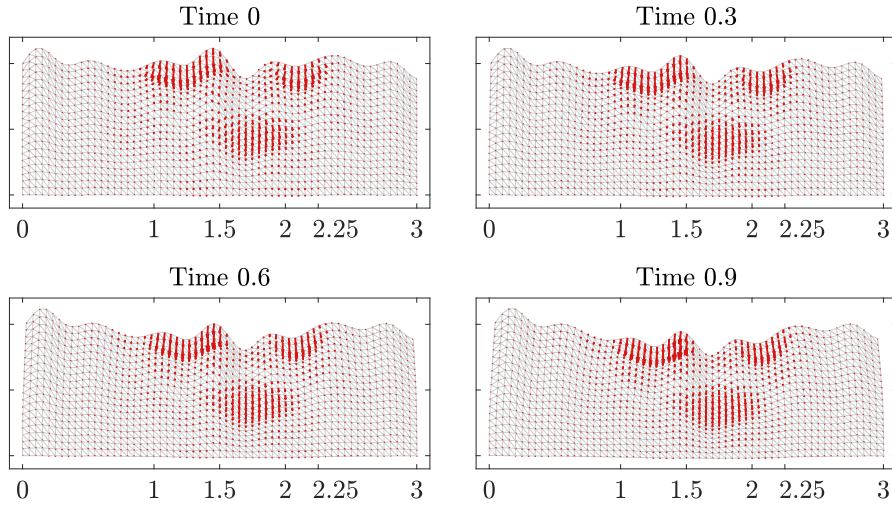
(D) Retrieved time-dependent yank (vectors scaled by 20).

FIGURE 5. Result of the free yank problem registering all layers.

enrolled in the BIOCARD cohort were all cognitively normal when the MRI scans were first acquired so that any observed atrophy in these brain volumes among those who progress to cognitive impairment provides significant information.

The layered structure on the source volume was inferred using the algorithm defined in [27, 36], which uses a normal propagation scheme between the lower and upper surfaces delimiting the shapes. The initial potential function estimated in this experiment is a sum of two compactly-supported functions such as defined in equation (12). Figure 10 summarizes

(A) Template.

(B) Potential at time zero.

(C) Deformed template.

(D) Time-dependent yank induced by the transported potential.
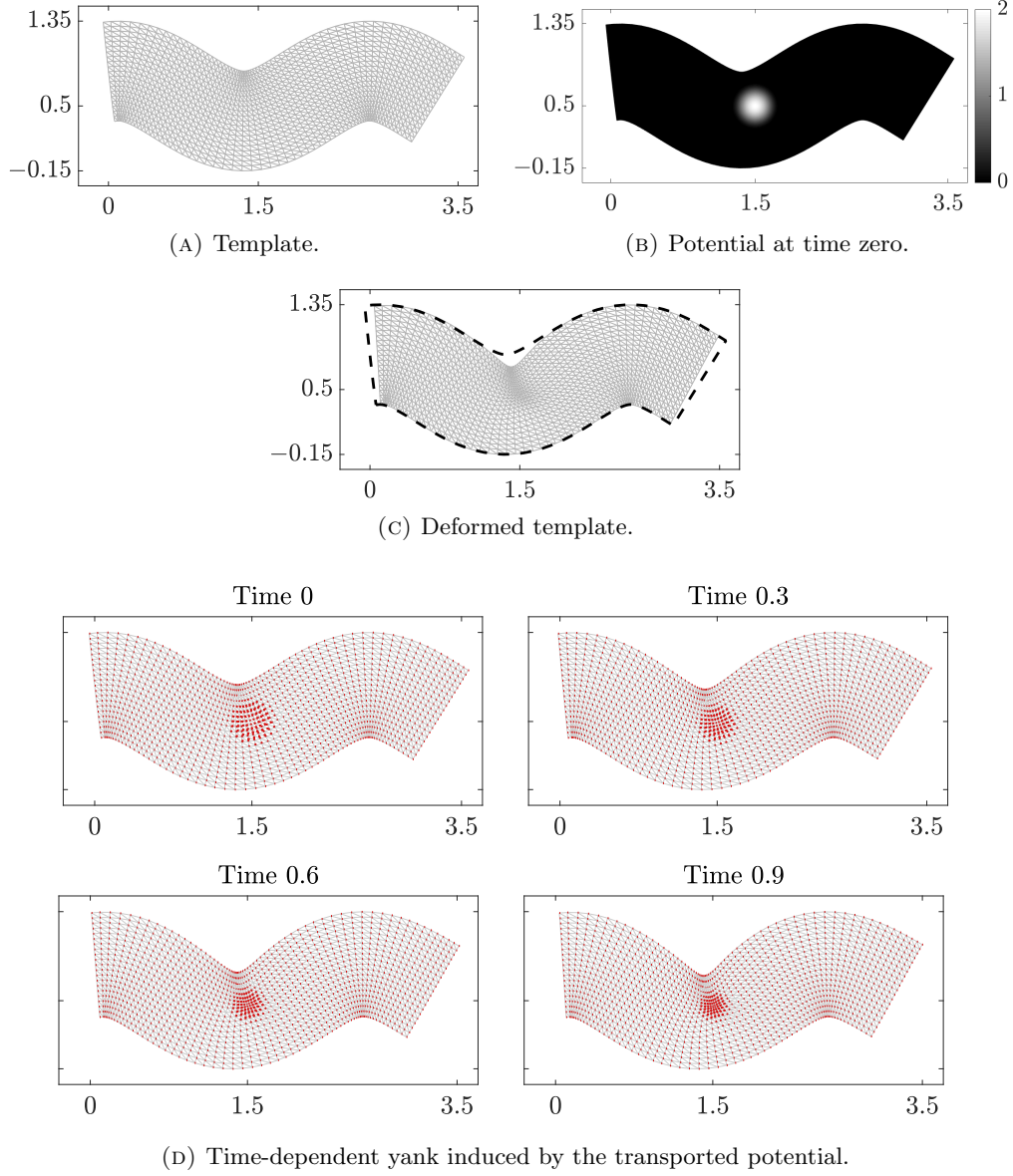
FIGURE 6. Simulated data for the parametrized yank problem.

the result that were obtained, with the location of the estimated potential and the resulting deformation. Note that these results are only provided here as an illustration of the proposed method, and we do not attempt to provide any new explanation yet on the pathogenesis of the disease. We hope, however, that this method may lead to new developments in this context in future work.
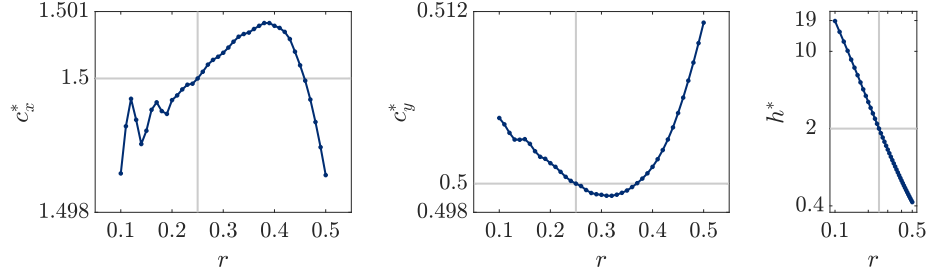
FIGURE 7. Sensitivity of minimizers with respect to the radius of potential. Gray lines indicate the true parameters. The slope of the log-log plot on the right is -2.37.
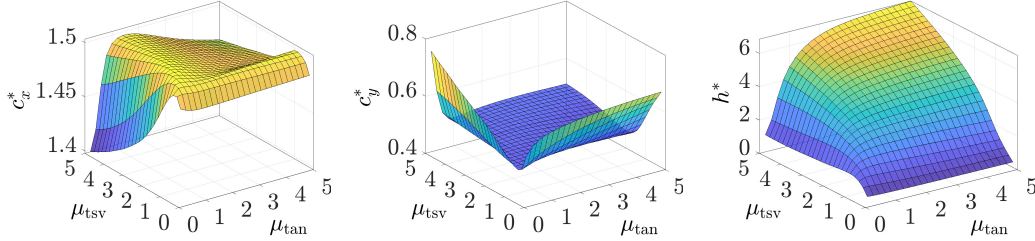

FIGURE 8. Sensitivity of minimizers with respect to elastic parameters.

6. PROOFS

We now prove Theorems 1 and 2. The two proofs being similar, it will be convenient to address together parts (i) of both theorems, and then parts (ii) together.

6.1. **Existence and uniqueness of solutions of controlled ODEs.** We will use the following version of local existence and uniqueness for controlled ordinary differential equations. In the following, we will say that a function u defined on $[0, T]$ with values in a metric space U is admissible if there exists a sequence of simple functions $u_n : [0, T] \to U$ such that $u_n(t)$ converges to $u(t)$ for almost every $t \in [0, T]$.

Theorem 3. *Let U be a metric space, and let O be an open subset of a Banach space $\mathbb{B}$. Let $F : U \times O \to \mathbb{B}$ be a continuous function that satisfies the following properties:*

(1) There exists a function $\gamma : U \to (0, \infty)$ such that, for all $u \in U$, $y \in O$:
$$\|F(u, y)\|_{\mathbb{B}} \leq \gamma(u) \left(1 + \|y\|_{\mathbb{B}}\right).$$

(2) For all $y_0 \in O$, there exists $r_{y_0} > 0$ and a function $\gamma_{y_0} : U \to (0, +\infty)$ such that for all $y, y' \in O$ with $\max(\|y - y_0\|_{\mathbb{B}}, \|y' - y_0\|_{\mathbb{B}}) \leq r_{y_0}$ and all $u \in U$
$$\|F(u, y) - F(u, y')\|_{\mathbb{B}} \leq \gamma_{y_0}(u) \|y - y'\|_{\mathbb{B}}. \tag{13}$$

Fix $T > 0$ and let $u : [0, T] \to U$ be admissible such that (i) $\gamma(u(t))$ is integrable on $[0, T]$ and (ii) for all $y_0 \in O$, $\gamma_{y_0}(u(t))$ is integrable on $[0, T]$. Then, for all $y_0 \in O$, there exists a largest $T_0 \leq T$ such that the ODE
$$\partial_t y(t) = F(u(t), y(t))$$
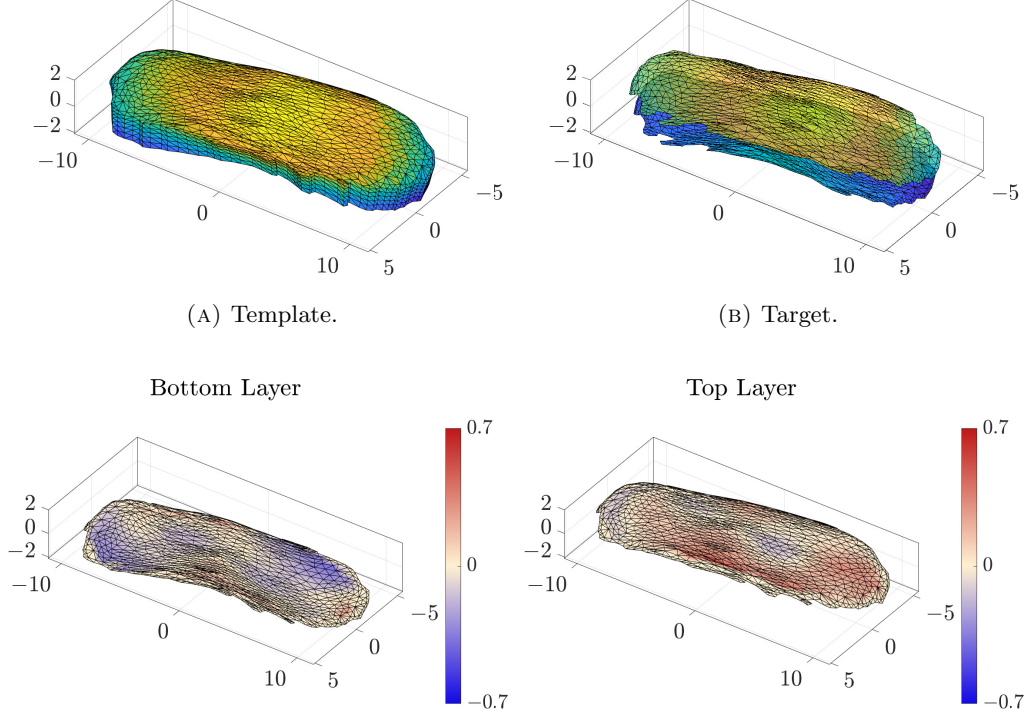
(A) Template.

(B) Target.

(C) Comparison between the template and target. The figures show the bottom and top layer of the template, and the color represents the z-coordinate of the template minus the one of the target.

FIGURE 9.   Entorhinal cortex volumes averaged over multiple patients from the BIOCARD dataset.

has a unique solution on $[0, T_0)$ satisfying $y(0) = y_0$.
In addition, one has

$$\sup_{t \in [0, T_0)} \|y(t)\|_{\mathbb{B}} \leq C \exp \left(\int_0^T \gamma(u(s)) ds \right). \tag{14}$$

where $C = \|y_0\|_{\mathbb{B}} + \int_0^T \gamma(u(s)) ds$ is a constant that only depends on y_0 and on the control u. Moreover, $y(t)$ has a limit in $\mathbb{B}$ when t tends to T_0 and, if $T_0 < T$, then $\lim_{t \to T_0} y(t) \notin O$.

Remark 5. By a solution of $\partial_t y(t) = F(u(t), y(t))$ over $[0, T_0)$ we mean a continuous function $y : [0.T_0) \to O$ satisfying

$$y(t) = y_0 + \int_0^t F(u(s), y(s)) ds$$

for all $t \in [0, T_0)$. The integral on the right-hand side is the Bochner integral. The fact that $s \mapsto F(u(s), y(s))$ is Bochner integrable is always true under the assumptions of Theorem 3, the proof being left to the reader.

(A) Support of potential.

(B) Deformation. The color represents the Jacobian det $D\varphi(t)$.

(C) Registration result. The figures show the bottom and top layer of the deformed template, and the color represents the z-coordinate of the deformed template minus the one of the target.
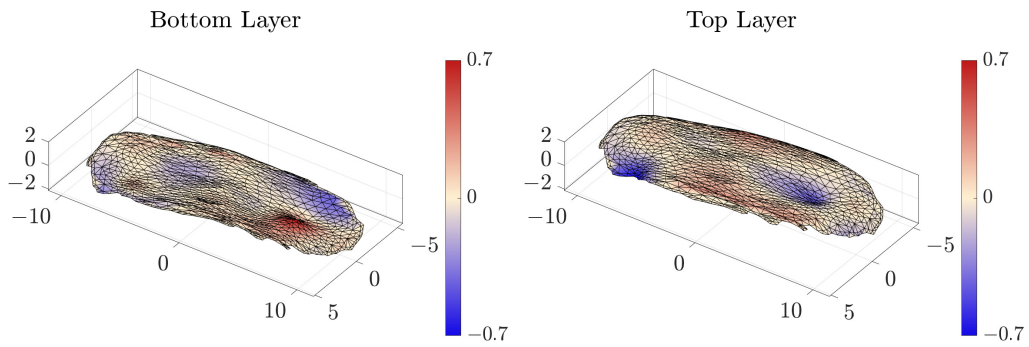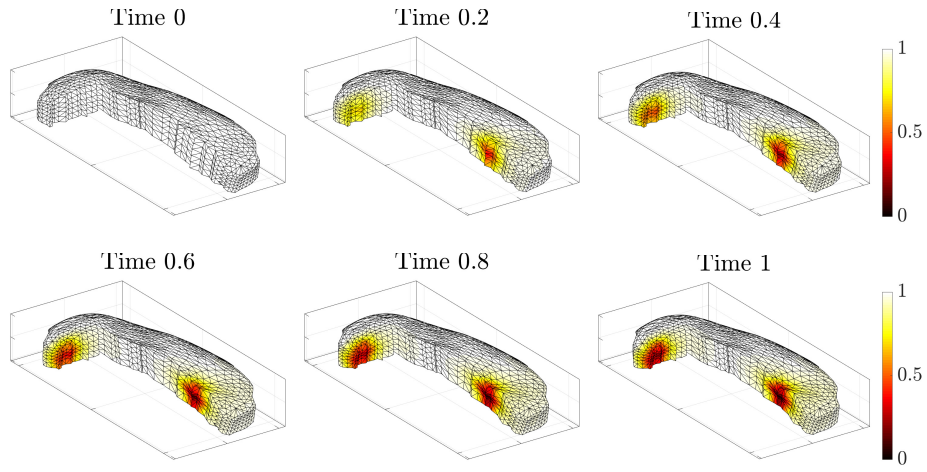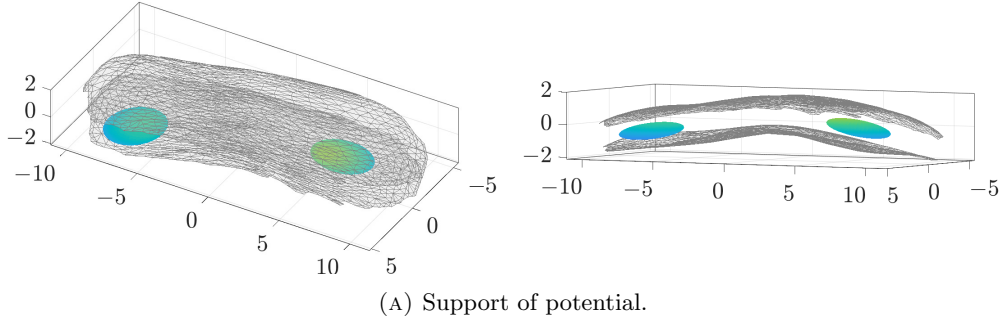
FIGURE 10.   Experimental results on averaged entorhinal cortex volumes.

Note that, letting $y(T_0) = \lim_{t \to T_0} y(t)$, we have, taking limits on both sides,

$$y(T_0) = y_0 + \int_0^{T_0} F(u(s), y(s))ds$$

Proof. The proof of the theorem is given here for completeness, and because the statement slightly deviates from that usually found in standard textbooks.

Fix $y_0 \in O$ and r_{y_0}, γ_{y_0} such that (13) is true. Let Ω denote the closed ball of center y_0 and radius r_{y_0} in $\mathbb{B}$. Reducing r_{y_0} if needed, assume that $\Omega \subset O$. Introduce a small $\eta > 0$, let $I_\eta = [0, \eta]$ and let $\mathcal{B}_\eta$ denote the complete metric space of continuous functions $y : I_\eta \to \Omega$ equipped with the metric $d(y, y') = \sup_{t \in [0, \eta]} \|y(t) - y'(t)\|_\mathbb{B}$. On this space, define, for $t \in I_\eta$,

$$\Gamma(y)(t) = y_0 + \int_0^t F(u(s), y(s))ds.$$

Then, if $y \in \mathcal{B}_\eta$,

$$\|\Gamma(y)(t) - y_0\|_\mathbb{B} \leq (1 + \|y_0\|_\mathbb{B} + r_{y_0}) \int_0^\eta \gamma(u(s))ds$$

so that Γ maps $\mathcal{B}_\eta$ onto itself as soon as $\int_0^\eta \gamma_0(u(s))ds \leq r_{y_0}/(1 + \|y_0\|_\mathbb{B} + r_{y_0})$. Moreover, for all $t \in I_\eta$ and all $y, y' \in \mathcal{B}_\eta$,

$$d(\Gamma(y) - \Gamma(y')) \leq \left(\int_0^\eta \gamma_{y_0}(u(s))ds \right) d(y, y'),$$

which shows that Γ is a contraction if $\int_0^\eta \gamma_{y_0}(u(s))ds < 1$. Taking η small enough, this shows that Γ has a unique fixed point in $\mathcal{B}_\eta$ and therefore proves local existence and uniqueness.

Now consider a solution y defined on $[0, T_0)$ with $T_0 \leq T$. For all $0 \leq t < T_0$:

$$\|y(t)\|_\mathbb{B} \leq \|y_0\|_\mathbb{B} + \int_0^t \gamma(u(s))(1 + \|y(s)\|_\mathbb{B})ds$$

$$\leq \|y_0\|_\mathbb{B} + \int_0^T \gamma(u(s))ds + \int_0^t \gamma(u(s))\|y(s)\|_\mathbb{B}ds,$$

which by Gronwall's inequality leads to

$$\|y(t)\|_\mathbb{B} \leq \left(\|y_0\|_\mathbb{B} + \int_0^T \gamma(u(s))ds \right) \exp \left(\int_0^T \gamma(u(s))ds \right)$$

and (14) follows by taking the supremum over all $t \in [0, T_0)$. Using this bound of solutions, we get that for all $t, t' \in [0, T_0)$:

$$\|y(t') - y(t)\|_\mathbb{B} \leq \int_t^{t'} \gamma(u(s))(1 + \|y(s)\|_\mathbb{B})ds \leq \widetilde{C} \int_t^{t'} \gamma(u(s))ds$$

for some constant $\widetilde{C}$ that depends on y_0 and u. This shows that y can be extended by continuity to $[0, T_0]$. Denote the limit by $y(T_0)$: if $T_0 < T$ and $y(T_0) \in O$, the solution can be extended further and we get a contradiction to the assumption that T_0 defines the largest interval. This concludes the proof of Theorem 3. $\square$

6.2. **Proof of Theorem 1(i).** We now return to our original problem and first note, by stating the following lemma, that $v(t)$ in (1) is well defined.

Lemma 1. *If $j \in V^*$ and $\varphi \in Diff_{id}^1(\mathbb{R}^3)$, then*

$$f(v) = \frac{\omega}{2} \|v\|_V^2 + \frac{1}{2} (A_\varphi v \,|\, v) - (j \,|\, v)$$

has a unique minimizer $v_{\varphi,j}$ in V given by $v_{\varphi,j} = L_\varphi^{-1} j$, where $L_\varphi = \omega K_V^{-1} + A_\varphi \in \mathscr{L}(V, V^*)$.

Proof. Since f is strictly convex and differentiable with

$$Df(v) = (\omega K_V^{-1} + A_\varphi)\, v - j = L_\varphi v - j,$$

the unique minimizer is characterized by $Df(v_{\varphi,j}) = 0$, i.e., L_φ is invertible and $v_{\varphi,j} = L_\varphi^{-1} j$. $\qquad\square$

System (1) can be rewritten as

$$\partial_t \varphi = F(j, \varphi) := v_{\varphi,j} \circ \varphi$$

and, letting $\varphi = id + h$ we want to apply Theorem 3 to the equation $\partial_t h = F(j, id + h)$, where we will take $U = V^*$, $\mathbb{B} = C_0^1(\mathbb{R}^d, \mathbb{R}^d)$ and $O = Diff_{id}^1(\mathbb{R}^d) - id$. We will show that the conditions for local existence are satisfied, and that, for any $T_0 \leq T$ such that a solution exists over $[0, T_0)$, the limit $\varphi(T_0)$ belongs to $Diff_{id}^1(\mathbb{R}^d)$, which will prove existence on the full interval. Note that, by assumption, j is Bochner integrable on $[0, T]$ and therefore admissible in the sense of Theorem 3.

The following lemma summarizes some useful inequalities.

Lemma 2.

(i) *If $v \in C_0^1(\mathbb{R}^3, \mathbb{R}^3)$ and $\varphi \in Diff_{id}^1(\mathbb{R}^3)$, then $v \circ \varphi \in C_0^1(\mathbb{R}^3, \mathbb{R}^3)$ and*

$$\|v \circ \varphi\|_{1,\infty} \leq (2 + \|\varphi - id\|_{1,\infty}) \|v\|_{1,\infty}.$$

(ii) *If $v \in C_0^2(\mathbb{R}^3, \mathbb{R}^3)$ and $\varphi, \psi \in Diff_{id}^1(\mathbb{R}^3)$, then*

$$\|v \circ \varphi - v \circ \psi\|_{1,\infty} \leq (2 + \|\psi - id\|_{1,\infty}) \|v\|_{2,\infty} \|\varphi - \psi\|_{1,\infty}.$$

(iii) *If $j \in V^*$ and $\varphi \in Diff_{id}^1(\mathbb{R}^3)$, then*

$$\|v_{\varphi,j}\|_V = \|L_\varphi^{-1} j\|_V \leq \frac{1}{\omega} \|j\|_{V^*},$$

i.e., $L_\varphi^{-1} \in \mathscr{L}(V^*, V)$ with $\|L_\varphi^{-1}\|_{\mathscr{L}(V^*, V)} \leq \frac{1}{\omega}$.

(iv) *If $j \in V^*$ and $\varphi, \psi \in Diff_{id}^1(\mathbb{R}^3)$, then*

$$\|L_\varphi^{-1} - L_\psi^{-1}\|_{\mathscr{L}(V^*, V)} \leq \frac{1}{\omega^2} \|A_\varphi - A_\psi\|_{\mathscr{L}(V, V^*)},$$

which implies

$$\|v_{\varphi,j} - v_{\psi,j}\|_V \leq \frac{1}{\omega^2} \|A_\varphi - A_\psi\|_{\mathscr{L}(V, V^*)} \|j\|_{V^*}.$$

Proof. The proofs of (i) and (ii) are straightforward applications of the chain rule and left to the reader. To show (iii), it is equivalent to prove that, for all $v \in V$, $\|v\|_V \leq (1/\omega)\,\|L_\varphi\,v\|_{V^*}$. We have, letting Id_V denote the identity operator on V,

$$\left(\frac{1}{\omega}\,\|L_\varphi\,v\|_{V^*}\right)^2 = \left(\frac{1}{\omega}\,\left\|K_V\left(\omega K_V^{-1} + A_\varphi\right)v\right\|_V\right)^2$$
$$= \frac{1}{\omega^2}\,\|(\omega\,Id_V + K_V A_\varphi)\,v\|_V^2$$
$$= \|v\|_V^2 + \frac{1}{\omega^2}\,\|K_V A_\varphi\,v\|_V^2 + \frac{2}{\omega}\,\langle v, K_V A_\varphi\,v\rangle_V$$
$$= \|v\|_V^2 + \frac{1}{\omega^2}\,\|K_V A_\varphi\,v\|_V^2 + \frac{2}{\omega}\,(A_\varphi\,v \mid v) \geq \|v\|_V^2,$$

where the last inequality follows from $(A_\varphi\,v \mid v) \geq 0$.

We now prove (iv), writing:

$$\|L_\varphi^{-1} - L_\psi^{-1}\|_{\mathscr{L}(V^*, V)} = \left\|L_\varphi^{-1}\left(L_\psi - L_\varphi\right)L_\psi^{-1}\right\|_{\mathscr{L}(V^*, V)}$$
$$= \left\|L_\varphi^{-1}\left(A_\psi - A_\varphi\right)L_\psi^{-1}\right\|_{\mathscr{L}(V^*, V)}$$
$$\leq \|L_\varphi^{-1}\|_{\mathscr{L}(V^*, V)}\,\|A_\varphi - A_\psi\|_{\mathscr{L}(V, V^*)}\,\|L_\psi^{-1}\|_{\mathscr{L}(V^*, V)}$$
$$\leq \frac{1}{\omega^2}\,\|A_\varphi - A_\psi\|_{\mathscr{L}(V, V^*)},$$

since (iii) implies that $\|L_\varphi^{-1}\|_{\mathscr{L}(V^*, V)} \leq (1/\omega)$. □

Corollary 1. *Let* $F(j, \varphi) = v_{\varphi,j} \circ \varphi$ *be defined on* $V^* \times Diff_{id}^1(\mathbb{R}^d)$. *Then, F is continuous and for all $j \in V^*$, and $\varphi \in Diff_{id}^1(\mathbb{R}^d)$,*

$$\|F(j, \varphi)\|_{1,\infty} \leq \frac{2c_V}{\omega}(1 + \|\varphi - id\|_{1,\infty})\|j\|_{V^*}$$

so that the assumption Theorem 3(1) holds for $\tilde{F} : (j, h) \mapsto F(j, id + h)$ *with* $\gamma(j) = (2c_V/\omega)\|j\|_{V^*}$.
Moreover, for all $j \in V^*$, *and* $\varphi, \psi \in Diff_{id}^1(\mathbb{R}^d)$

$$\|F(j, \varphi) - F(j, \psi)\|_{1,\infty} \leq C_\psi\left(\|\varphi - \psi\|_{1,\infty} + \|A_\varphi - A_\psi\|_{\mathscr{L}(V, V^*)}\right)\|j\|_{V^*}.$$

Thus, if A_φ is locally Lipschitz, so is F and $\tilde{F}$, and the assumption Theorem 3(2) holds.

Proof. We have

$$\|F(j, \varphi)\|_{1,\infty} \leq (2 + \|\varphi - id\|_{1,\infty})\|v_{\varphi,j}\|_{1,\infty}$$
$$\leq c_V(2 + \|\varphi - id\|_{1,\infty})\|v_{\varphi,j}\|_V$$
$$\leq \frac{c_V}{\omega}(2 + \|\varphi - id\|_{1,\infty})\|j\|_{V^*}.$$

This inequality also shows the continuity of F in j, since $F(j, \varphi) = (L_\varphi^{-1}j) \circ \varphi$ is linear in j.

Similarly

$$
\begin{aligned}
\|F(j,\varphi) - F(j,\psi)\|_{1,\infty} &\leq \|v_{\varphi,j} \circ \varphi - v_{\varphi,j} \circ \psi\|_{1,\infty} + \|v_{\varphi,j} \circ \psi - v_{\psi,j} \circ \psi\|_{1,\infty} \\
&\leq (2 + \|\psi - id\|_{1,\infty})\|\varphi - \psi\|_{1,\infty}\|v_{\varphi,j}\|_{2,\infty} \\
&\quad + (2 + \|\psi - id\|_{1,\infty})\|v_{\varphi,j} - v_{\psi,j}\|_{1,\infty} \\
&\leq \frac{c_V}{\omega}(2 + \|\psi - id\|_{1,\infty})\|\varphi - \psi\|_{1,\infty}\|j\|_{V^*} \\
&\quad + \frac{1}{\omega^2}(2 + \|\psi - id\|_{1,\infty})\|A_\varphi - A_\psi\|_{\mathscr{L}(V,V^*)}\|j\|_{V^*}.
\end{aligned}
$$

Since $F(j,\varphi)$ is continuous and linear in j and continuous in φ, we know that F is continuous. $\qquad \square$

Corollary 1 therefore implies that (1) has a unique local solution as soon as $j(t)$ is integrable. To conclude the proof of (i) in Theorem 1, it suffices to show that any solution on an interval $[0, T_0)$ is such that $\varphi(T_0) := \lim_{t \uparrow T_0} \varphi(t) \in Diff_{id}^1(\mathbb{R}^d)$. This is true because, if one lets $w(t) = v_{\varphi(t),j(t)}$, then $w \in L^1([0, T_0], V)$ and φ is, by construction, the flow associated to the ordinary differential equation $\partial_t z = w(t, z)$, i.e., it satisfies $\partial_t \varphi(t, x) = w(t, \varphi(t, x))$. This shows that (see, e.g., [33] Chap. 8) $\varphi \in C([0, T_0], Diff_{id}^2(\mathbb{R}^3))$, which completes the proof of part (i) of Theorem 1.

In particular, for $t \in [0, T_0]$, one has $\varphi(t, \cdot)^{-1} = \psi(t, \cdot)$ where ψ is the flow associated with the equation $\partial_s z = \tilde{w}^{(t)}(s, z)$, with $\tilde{w}^{(t)}(s) = -v_{\varphi(t-s),j(t-s)}$. Note that we have not defined w at time T_0 (or $\tilde{w}$ at time 0), which is not a problem since these time-dependent vector fields only need to be defined almost everywhere (in t) for the result to hold. (One can actually show using Cauchy sequences that $w(t)$ has a limit when t tends to T_0 anyway).

We also point out that, using the inequalities of Lemma 2, the transcription of (14) to the present case becomes $\|\varphi(t) - id\|_{1,\infty} \leq B_j$ with

$$
B_j = \frac{2c_v}{\omega}\|j\|_{\mathcal{X}_{V^*,T}^1} \exp\Big(\frac{c_V}{\omega}\|j\|_{\mathcal{X}_{V^*,T}^1}\Big). \tag{15}
$$

(here, the initial condition is always $\varphi(0, \cdot) = id$) and thus B_j only depends on j.

We also have $\|\varphi^{-1}(t) - id\|_{1,\infty} \leq B_j$. This can be proved for each t by applying Theorem 3 to $F(\tilde{w}, \psi) = \tilde{w} \circ \psi$, with $U = V$, which satisfies the hypotheses with $\gamma(\tilde{w}) = c_V\|\tilde{w}\|_V$. To obtain the same constant B_j, one only needs to notice that, for all s, $\|\tilde{w}^{(t)}(s)\|_V = \|w(t-s)\|_V$

We summarize this discussion in the next lemma.

Lemma 3. *Suppose that $j \in \mathcal{X}_{V^*,T}^1$. If $\varphi \in C([0, T_0], Diff_{id}^1(\mathbb{R}^3))$ is a local solution to system (1) for some $T_0 \leq T$, then $\|\varphi(t) - id\|_{1,\infty} \leq B_j$ and $\|\varphi^{-1}(t) - id\|_{1,\infty} \leq B_j$ for all $t \in [0, T_0]$, where B_j is defined in equation (15).*

Moreover, the local solution φ is actually in $C([0, T_0], Diff_{id}^2(\mathbb{R}^3))$ and there exists a constant C_j such that

$$
\|D^2\varphi(t)\|_\infty \leq C_j \exp\Big(\frac{c_V}{\omega}\|j\|_{\mathcal{X}_{V^*,T}^1}\Big) \tag{16}
$$

for all $t \in [0, T_0]$.

Only the last inequality remains to be shown. We have

$$|D^2\varphi(t,x)| \leq \int_0^t \Big(|D^2 v_{\varphi(s),j(s)}(\varphi(s,x))| \, |D\varphi(s,x)|^2$$
$$+ |Dv_{\varphi(s),j(s)}(\varphi(s,x))| \, |D^2\varphi(s,x)| \Big) \, ds, \tag{17}$$
$$\leq \frac{c_V}{\omega} \|j\|_{\mathcal{X}^1_{V^*,T}} \|D\varphi(t)\|_\infty^2 + \frac{c_V}{\omega} \int_0^t \|j(s)\|_{V^*} |D^2\varphi(s,x)| \, ds$$

and inequality (16) follows from Gronwall's lemma, since $\|D\varphi(t)\|_\infty^2 \leq (1 + B_j)^2$.

6.3. **Proof of Theorem 2(i).** Denote $v_{\varphi,\theta} = v_{\varphi,j(\varphi,\theta)}$ and let

$$G_\theta(\varphi) = v_{\varphi,\theta} \circ \varphi.$$

We only need to apply the standard existence theorem for the ODE $\partial_t \varphi = G_\theta(\varphi)$. For this, it is sufficient to prove that, for any $\theta \in \Theta$,

(1) There exists $\gamma > 0$ such that, for all $\varphi \in Diff_{id}^1(\mathbb{R}^d)$:

$$\|G_\theta(\varphi)\|_{1,\infty} \leq \gamma(1 + \|\varphi - id\|_{1,\infty}) .$$

(2) For all $\varphi_0 \in Diff_{id}^1(\mathbb{R}^d)$, there exists $r_{\varphi_0} > 0$ and $\gamma_{\varphi_0} > 0$ such that for all $\varphi, \psi \in Diff_{id}^1(\mathbb{R}^d)$ with $\max(\|\varphi - \varphi_0\|_\mathbb{B}, \|\psi - \varphi_0\|_\mathbb{B}) \leq r_{\varphi_0}$

$$\|G_\theta(\varphi) - G_\theta(\psi)\|_{1,\infty} \leq \gamma_{\varphi_0} \|\varphi - \psi\|_{1,\infty} .$$

These properties are easily deduced from Lemma 2 and the boundedness and Lipschitz assumptions made on $j(\varphi, \theta)$, and we skip the argument.

6.4. **Proof of Theorem 1(ii).** Given $j \in \mathcal{X}^2_{V^*,T} \subset \mathcal{X}^1_{V^*,T}$, we have proved that system (1) has a unique solution $\varphi_j \in C([0,T], Diff_{id}^2(\mathbb{R}^3))$. Denote the well-defined objective function by

$$f(j) = \int_0^T (j(t) \,|\, v_{\varphi_j(t),j(t)}) \, dt + \rho(\varphi_j(T, M_0), M_\text{targ}).$$

To prove the existence of minimizers of f, we show that minimizing sequences of f are bounded and f is weakly sequentially lower semicontinuous. Since $\mathcal{X}^2_{V^*,T}$ is a Hilbert space, the existence of minimizers will follow by applying the direct method of the calculus of variations.

Lemma 4. *Minimizing sequences of f are bounded.*

Proof. Let $(j_n)_{n=1}^\infty$ be a minimizing sequence of f. We denote for short $v_n(t) := v_{\varphi_{j_n}(t),j_n(t)}$. Note that the solution of $j \equiv 0$ is $\varphi_j \equiv id$, so we can assume $f(j_n) \leq f(0) = \rho(M_0, M_\text{targ})$ without loss of generality. Using Lemma 1, we have $j_n(t) = (\omega K_V^{-1} + A_{\varphi_{j_n}(t)}) v_n(t)$. It follows that

$$\rho(M_0, M_\text{targ}) \geq f(j_n) \geq \int_0^T (j_n(t) \,|\, v_n(t)) \, dt$$
$$\geq \int_0^T \omega \, (K_V^{-1} v_n(t) \,|\, v_n(t)) \, dt \tag{18}$$
$$= \omega \int_0^T \|v_n(t)\|_V^2 \, dt \geq \frac{\omega}{T} \left(\int_0^T \|v_n(t)\|_V \, dt \right)^2$$

From Theorem 3 (applied to $F(v, h) = v \circ (id + h)$ and $U = V$), we know that the boundedness of $\int_0^T \|v_n(t)\|_V \, dt$ implies the boundedness of solutions, i.e., there exists a constant B such that $\|\varphi_{j_n}(t) - id\|_{1,\infty} \leq B$ for all $t \in [0, T]$ and $n \in \mathbb{N}$. Since $\varphi \mapsto A_\varphi$ is Lipschitz with respect to the seminorm $\| \cdot \|_{1,\infty}^{M_0}$ on $\mathfrak{S}_B$, denoting the Lipschitz constant by $\ell_A(B)$ leads to

$$\|A_{\varphi_{j_n}(t)}\|_{\mathscr{L}(V, V^*)} \leq \|A_{id}\|_{\mathscr{L}(V, V^*)} + \ell_A \, \|\varphi_{j_n}(t) - id\|_{1,\infty}^{M_0} \leq C_B.$$

Now we return to inequality (18) and write

$$\rho(M_0, M_{\text{targ}}) \geq \omega \int_0^T \|v_n(t)\|_V^2 \, dt$$

$$\geq \omega \int_0^T \left(\frac{\|j_n(t)\|_{V^*}}{\|\omega K_V^{-1} + A_{\varphi_{j_n}(t)}\|_{\mathscr{L}(V, V^*)}} \right)^2 dt$$

$$\geq \omega \int_0^T \left(\frac{\|j_n(t)\|_{V^*}}{\omega + C_B} \right)^2 dt = C_B \, \|j_n\|_{\mathcal{X}_{V^*, T}^2}^2,$$

where we have used the fact that K_V^{-1} is an isometry from V to V^* in the third inequality. The above inequality shows that a minimizing sequence $(j_n)_{n=1}^\infty$ is bounded. $\square$

To prove that f is weakly sequentially lower semicontinuous, we separate the two terms in f and show in Lemmas 6 and 7 respectively that the first term $j \mapsto \int_0^T (j(t) \,|\, v_{\varphi_j(t), j(t)}) \, dt$ and the second term $j \mapsto \rho(\varphi_j(T, M_0), M_{\text{targ}})$ are both weakly sequentially lower semicontinuous.

Let $j_n \rightharpoonup j$ in $\mathcal{X}_{V^*, T}^2$. We first derive some preliminary bounds that will be used in the following Lemmas 5 to 7. Since $j_n \rightharpoonup j$, there exists $J > 0$ such that $\|j_n\|_{\mathcal{X}_{V^*, T}^2} \leq J$ for all $n \in \mathbb{N}$. It follows that

$$\|j\|_{\mathcal{X}_{V^*, T}^2} \leq \liminf_{n \to \infty} \|j_n\|_{\mathcal{X}_{V^*, T}^2} \leq J.$$

For the solution φ_{j_n}, Lemma 3 shows that for every $t \in [0, T]$

$$\|\varphi_{j_n}(t) - id\|_{1,\infty} \leq \frac{2c_V}{\omega} \, \|j_n\|_{\mathcal{X}_{V^*, T}^1} \, \exp\left(\frac{c_V}{\omega} \|j_n\|_{\mathcal{X}_{V^*, T}^1} \right),$$

so

$$\|\varphi_{j_n}(t) - id\|_{1,\infty} \leq \frac{2c_V}{\omega} \, J\sqrt{T} \, \exp\left(\frac{c_V}{\omega} J\sqrt{T} \right) =: B_J.$$

Similarly, we have

$$\|\varphi_j(t) - id\|_{1,\infty} \leq \frac{2c_V}{\omega} \, \|j\|_{\mathcal{X}_{V^*, T}^1} \, \exp\left(\frac{c_V}{\omega} \|j\|_{\mathcal{X}_{V^*, T}^1} \right)$$

$$\leq \frac{2c_V}{\omega} \, J\sqrt{T} \, \exp\left(\frac{c_V}{\omega} J\sqrt{T} \right) = B_J.$$

Still from Lemma 3, it also holds that

$$\|\varphi_{j_n}^{-1}(t) - id\|_{1,\infty} \leq B_J \quad \text{and} \quad \|\varphi_j^{-1}(t) - id\|_{1,\infty} \leq B_J.$$

We then have $(\varphi_{j_n})_{n=1}^\infty \subset \mathfrak{S}_{B_J}$ and $\varphi_j \in \mathfrak{S}_{B_J}$, where $\mathfrak{S}_{B_J}$ is defined in the statement of the theorem.

The following lemma is a preliminary step towards Lemmas 6 and 7, which prove the weakly sequentially lower semicontinuity of f.

Lemma 5. *If $j_n \rightharpoonup j$ in $\mathcal{X}_{V^*, T}^2$, then $\|\varphi_{j_n}(t) - \varphi_j(t)\|_{1,\infty}^{M_0} \to 0$ for all $t \in [0, T]$.*

Proof. Note that

$$\varphi_{j_n}(t,x) - \varphi_j(t,x)$$

$$= \int_0^t \left(v_{\varphi_{j_n}(s), j_n(s)}(\varphi_{j_n}(s,x)) - v_{\varphi_j(s), j(s)}(\varphi_j(s,x)) \right) ds$$

$$= \int_0^t \left(\left(L_{\varphi_{j_n}(s)}^{-1} j_n(s) \right) (\varphi_{j_n}(s,x)) - \left(L_{\varphi_j(s)}^{-1} j_n(s) \right) (\varphi_{j_n}(s,x)) \right) ds$$

$$+ \int_0^t \left(\left(L_{\varphi_j(s)}^{-1} j_n(s) \right) (\varphi_{j_n}(s,x)) - \left(L_{\varphi_j(s)}^{-1} j_n(s) \right) (\varphi_j(s,x)) \right) ds$$

$$+ \int_0^t \left(\left(L_{\varphi_j(s)}^{-1} j_n(s) \right) (\varphi_j(s,x)) - \left(L_{\varphi_j(s)}^{-1} j(s) \right) (\varphi_j(s,x)) \right) ds$$

$$=: I_{1,n}(t) + I_{2,n}(t) + \Lambda_n(t)$$

Taking $\| \cdot \|_{1,\infty}^{M_0}$ on both sides, we will show that

$$\|I_{1,n}(t)\|_{1,\infty}^{M_0} + \|I_{2,n}(t)\|_{1,\infty}^{M_0} \leq C_J \left(\int_0^t \left(\|\varphi_{j_n}(s) - \varphi_j(s)\|_{1,\infty}^{M_0} \right)^2 ds \right)^{\frac{1}{2}}, \qquad (19)$$

and that

$$\lim_{n \to \infty} \|\Lambda_n(t)\|_{1,\infty}^{M_0} = 0 \quad \text{for all } t \in [0,T]. \qquad (20)$$

Identities (19) and (20) combined with Gronwall's lemma will then lead to $\|\varphi_{j_n}(t) - \varphi_j(t)\|_{1,\infty}^{M_0} \to 0$ for all $t \in [0,T]$.

We estimate $\|I_{1,n}(t)\|_{1,\infty}^{M_0}$ as follows.

$$\|I_{1,n}(t)\|_{1,\infty}^{M_0}$$

$$\leq \int_0^t \left\| \left(L_{\varphi_{j_n}(s)}^{-1} j_n(s) \right) \circ \varphi_{j_n}(s) - \left(L_{\varphi_j(s)}^{-1} j_n(s) \right) \circ \varphi_{j_n}(s) \right\|_{1,\infty} ds$$

$$\leq \int_0^t (2 + \|\varphi_{j_n}(s) - id\|_{1,\infty}) \left\| L_{\varphi_{j_n}(s)}^{-1} j_n(s) - L_{\varphi_j(s)}^{-1} j_n(s) \right\|_{1,\infty} ds \quad \text{(Lemma 2(i))}$$

$$\leq \int_0^t (2 + B_J) \frac{c_V}{\omega^2} \|A_{\varphi_{j_n}(s)} - A_{\varphi_j(s)}\|_{\mathscr{L}(V,V^*)} \|j_n(s)\|_{V^*} ds \quad \text{(Lemma 2(iv))}$$

Since $\varphi \mapsto A_\varphi$ is Lipschitz on $\mathfrak{S}_{B_J}$ with respect to $\| \cdot \|_{1,\infty}^{M_0}$, denoting the Lipschitz constant by $\ell_A(B_J)$ leads to

$$\|I_{1,n}(t)\|_{1,\infty}^{M_0} \leq \frac{c_V}{\omega^2} (2 + B_J) \int_0^t \ell_A \|\varphi_{j_n}(s) - \varphi_j(s)\|_{1,\infty}^{M_0} \|j_n(s)\|_{V^*} ds \qquad (21)$$

$$\leq \frac{c_V}{\omega^2} (2 + B_J) \ell_A \left(\int_0^t \left(\|\varphi_{j_n}(s) - \varphi_j(s)\|_{1,\infty}^{M_0} \right)^2 ds \right)^{\frac{1}{2}} \|j_n\|_{\mathcal{X}_{V^*,T}^2}$$

$$\leq C_J \left(\int_0^t \left(\|\varphi_{j_n}(s) - \varphi_j(s)\|_{1,\infty}^{M_0} \right)^2 ds \right)^{\frac{1}{2}}.$$

We now pass to $\|I_{2,n}(t)\|_{1,\infty}^{M_0}$. Similarly to Lemma 2(ii), we have

$$\|v \circ \varphi - v \circ \psi\|_{1,\infty}^{M_0} \leq (2 + \|\psi - id\|_{1,\infty}^{M_0}) \|v\|_{2,\infty} \|\varphi - \psi\|_{1,\infty}^{M_0}.$$

It follows that

$$\|I_{2,n}(t)\|_{1,\infty}^{M_0}$$

$$\leq \int_0^t \left\| \left(L_{\varphi_j(s)}^{-1} j_n(s) \right) \circ \varphi_{j_n}(s) - \left(L_{\varphi_j(s)}^{-1} j_n(s) \right) \circ \varphi_j(s) \right\|_{1,\infty}^{M_0} ds$$

$$\leq \int_0^t \left(2 + \|\varphi_j(s) - id\|_{1,\infty}^{M_0} \right) \|L_{\varphi_j(s)}^{-1} j_n(s)\|_{2,\infty} \|\varphi_{j_n}(s) - \varphi_j(s)\|_{1,\infty}^{M_0} ds$$

$$\leq \int_0^t (2 + B_J) \frac{c_V}{\omega} \|j_n(s)\|_{V^*} \|\varphi_{j_n}(s) - \varphi_j(s)\|_{1,\infty}^{M_0} ds \qquad (22)$$

$$\leq C_J \left(\int_0^t \left(\|\varphi_{j_n}(s) - \varphi_j(s)\|_{1,\infty}^{M_0} \right)^2 ds \right)^{\frac{1}{2}}.$$

We proceed to show that (20) holds. To simplify notations, define $u_n : \mathbb{R}^3 \to \mathbb{R}^3$ and $u : \mathbb{R}^3 \to \mathbb{R}^3$ by

$$u_n(x) = \int_0^t \left(L_{\varphi_j(s)}^{-1} j_n(s) \right) \circ \varphi_j(s, x) \, ds \quad \text{and} \quad u(x) = \int_0^t \left(L_{\varphi_j(s)}^{-1} j(s) \right) \circ \varphi_j(s, x) \, ds$$

and prove that $\|u_n - u\|_\infty^{M_0}$ and $\|Du_n - Du\|_\infty^{M_0}$ converge to 0 as $n \to \infty$. We aim to prove pointwise convergence, uniform boundedness, and equicontinuity of the two sequences, so as to invoke the Arzelà–Ascoli theorem. Given $x \in \mathbb{R}^3$, we define linear operators $\mathcal{L}_x : \mathcal{X}_{V^*, T}^2 \to \mathbb{R}^3$ and $\widetilde{\mathcal{L}}_x : \mathcal{X}_{V^*, T}^2 \to \mathbb{R}^{3 \times 3}$ by

$$\mathcal{L}_x j' = \int_0^t \left(L_{\varphi_j(s)}^{-1} j'(s) \right) \circ \varphi_j(s, x) \, ds \quad \text{and} \quad \widetilde{\mathcal{L}}_x j' = \int_0^t D\left(L_{\varphi_j(s)}^{-1} j'(s) \circ \varphi_j(s, x) \right) ds.$$

Note that

$$|\mathcal{L}_x j'| + |\widetilde{\mathcal{L}}_x j'| \leq \int_0^t \left\| \left(L_{\varphi_j(s)}^{-1} j'(s) \right) \circ \varphi_j(s) \right\|_{1,\infty} ds \leq \frac{c_V \sqrt{T}}{\omega} (2 + B_J) \|j'\|_{\mathcal{X}_{V^*, T}^2},$$

so both $\mathcal{L}_x$ and $\widetilde{\mathcal{L}}_x$ are bounded linear operators for all $x \in \mathbb{R}^3$. Since $j_n \rightharpoonup j$, pointwise convergence of $(u_n)_{n=1}^\infty$ and $(Du_n)_{n=1}^\infty$ now follows from

$$u_n(x) = \mathcal{L}_x j_n \to \mathcal{L}_x j = u(x) \quad \text{and} \quad Du_n(x) = \widetilde{\mathcal{L}}_x j_n \to \widetilde{\mathcal{L}}_x j = Du(x).$$

We also have

$$|u_n(x)| + |Du_n(x)| = |\mathcal{L}_x j_n| + |\widetilde{\mathcal{L}}_x j_n| \leq \frac{c_V \sqrt{T}}{\omega} (2 + B_J) \|j_n\|_{\mathcal{X}_{V^*, T}^2} \leq C_J,$$

which shows that the two sequences are uniformly bounded. The sequence $(u_n)_{n=1}^\infty$ is equicontinuous on $\mathbb{R}^3$ because

$$|u_n(x) - u_n(y)| \leq \int_0^t \left\| D\left(L_{\varphi_j(s)}^{-1} j_n(s) \right) \right\|_\infty \|D\varphi_j(s)\|_\infty |x - y| \, ds \leq C_J |x - y|.$$

The sequence $(Du_n)_{n=1}^\infty$ is equicontinuous on $\mathbb{R}^3$ because

$$|Du_n(x) - Du_n(y)|$$

$$\leq \int_0^t \left(\left| \left(D\left(L_{\varphi_j(s)}^{-1} j_n(s)\right) \circ \varphi_j(s,x)\right) D\varphi_j(s,x) \right. \right.$$

$$- \left. \left(D\left(L_{\varphi_j(s)}^{-1} j_n(s)\right) \circ \varphi_j(s,x)\right) D\varphi_j(s,y) \right|$$

$$+ \left| \left(D\left(L_{\varphi_j(s)}^{-1} j_n(s)\right) \circ \varphi_j(s,x)\right) D\varphi_j(s,y) \right.$$

$$- \left. \left. \left(D\left(L_{\varphi_j(s)}^{-1} j_n(s)\right) \circ \varphi_j(s,y)\right) D\varphi_j(s,y) \right| \right) ds$$

$$\leq \int_0^t \left(\left\| D\left(L_{\varphi_j(s)}^{-1} j_n(s)\right) \right\|_\infty \|D^2\varphi_j(s)\|_\infty |x-y| \right.$$

$$+ \left. \left\| D^2\left(L_{\varphi_j(s)}^{-1} j_n(s)\right) \right\|_\infty \|D\varphi_j(s)\|_\infty |x-y| \, \|D\varphi_j(s)\|_\infty \right) ds$$

$$\leq C_J |x-y|,$$

where we have used $\|D^2\varphi_j(s)\|_\infty \leq C_J$ by (16). From the Arzelà–Ascoli theorem, we know that every subsequence of $(u_n)_{n=1}^\infty$ has a further subsequence that converges uniformly to u on M_0, which implies $\|u_n - u\|_\infty^{M_0} \to 0$. Applying the same argument to the sequence $(Du_n)_{n=1}^\infty$ gives $\|Du_n - Du\|_\infty^{M_0} \to 0$.

In summary, we have proved (19) and (20), which lead to

$$\|\varphi_{j_n}(t) - \varphi_j(t)\|_{1,\infty}^{M_0} \leq \|I_{1,n}(t)\|_{1,\infty}^{M_0} + \|I_{2,n}(t)\|_{1,\infty}^{M_0} + \|\Lambda_n(t)\|_{1,\infty}^{M_0}$$

$$\leq \lambda_n(t) + C_J \left(\int_0^t \left(\|\varphi_{j_n}(s) - \varphi_j(s)\|_{1,\infty}^{M_0} \right)^2 ds \right)^{\frac{1}{2}}, \tag{23}$$

where $\lambda_n(t) = \|\Lambda_n(t)\|_{1,\infty}^{M_0} \to 0$ as $n \to \infty$. This implies

$$\left(\|\varphi_{j_n}(t) - \varphi_j(t)\|_{1,\infty}^{M_0} \right)^2 \leq 2\lambda_n^2(t) + \int_0^t 2 C_J^2 \left(\|\varphi_{j_n}(s) - \varphi_j(s)\|_{1,\infty}^{M_0} \right)^2 ds.$$

By Gronwall's lemma, we finally obtain

$$\left(\|\varphi_{j_n}(t) - \varphi_j(t)\|_{1,\infty}^{M_0} \right)^2 \leq 2\lambda_n^2(t) + \int_0^t 4\lambda_n^2(s) C_J^2 \exp\left(2 C_J^2(t-s)\right) ds. \tag{24}$$

Note that

$$\lambda_n(t) \leq \left\| \int_0^t \left(\left(L_{\varphi_j(s)}^{-1} j_n(s)\right) \circ \varphi_j(s) - \left(L_{\varphi_j(s)}^{-1} j(s)\right) \circ \varphi_j(s) \right) ds \right\|_{1,\infty}$$

$$\leq \int_0^t (2 + \|\varphi_j(s) - id\|_{1,\infty}) \left\| L_{\varphi_j(s)}^{-1} j_n(s) - L_{\varphi_j(s)}^{-1} j(s) \right\|_{1,\infty} ds \tag{25}$$

$$\leq \int_0^t (2 + B_J) \frac{c_V}{\omega} \left(\|j_n(s)\|_{V^*} + \|j(s)\|_{V^*} \right) ds \leq C_J,$$

so $\lambda_n(t)$ is uniformly bounded in n and t. The dominated convergence theorem then shows that the right hand integral of (24) converges to 0 as $n \to \infty$ and thus

$$\|\varphi_{j_n}(t) - \varphi_j(t)\|_{1,\infty}^{M_0} \to 0 \quad \text{as} \quad n \to \infty,$$

which completes the proof. $\square$

We immediately have the following lemma as a corollary.

Lemma 6. *The second term $j' \mapsto \rho(\varphi_{j'}(T, M_0), M_{\text{targ}})$ in f is weakly sequentially continuous; hence it is weakly sequentially lower semicontinuous.*

Proof. Lemma 5 shows, in particular at $t = T$, that $j_n \rightharpoonup j$ implies $\|\varphi_{j_n}(T) - \varphi_j(T)\|_{1,\infty}^{M_0} \to 0$. Since the discrepancy function ρ is continuous on $\mathcal{M}$ with respect to $\|\cdot\|_{1,\infty}$, we have $\rho(\varphi_{j_n}(T, M_0), M_{\text{targ}}) \to \rho(\varphi_j(T, M_0), M_{\text{targ}})$, yielding that $j' \mapsto \rho(\varphi_{j'}(T, M_0), M_{\text{targ}})$ is weakly sequentially continuous. $\square$

Lemma 7. *The first term $j' \mapsto \int_0^T (j'(t) \mid v_{\varphi_{j'}(t), j'(t)}) \, dt$ in f is weakly sequentially lower semicontinuous.*

Proof. Let $j_n \rightharpoonup j$ in $\mathcal{X}_{V^*, T}^2$. Denote $v_n(t) := v_{\varphi_{j_n}(t), j_n(t)}$ and $v(t) := v_{\varphi_j(t), j(t)}$. We first show that $v_n, v \in \mathcal{X}_{V, T}^2$ for all $n \in \mathbb{N}$ and $v_n \rightharpoonup v$ in $\mathcal{X}_{V, T}^2$. Lemma 2(iii) gives

$$\int_0^T \|v_n(t)\|_V^2 \, dt = \int_0^T \|L_{\varphi_{j_n}(t)}^{-1} j_n(t)\|_V^2 \, dt \leq \frac{1}{\omega^2} \|j_n\|_{\mathcal{X}_{V^*, T}}^2,$$

so $v_n \in \mathcal{X}_{V, T}^2$. Moreover,

$$\|v_n\|_{\mathcal{X}_{V, T}^2} \leq \frac{1}{\omega} \|j_n\|_{\mathcal{X}_{V^*, T}^2} \leq \frac{J}{\omega}$$

for all $n \in \mathbb{N}$. The same argument shows that $v \in \mathcal{X}_{V, T}^2$. To see $v_n \rightharpoonup v$ in $\mathcal{X}_{V, T}^2$, consider an arbitrary $\mu \in (\mathcal{X}_{V, T}^2)^* \simeq \mathcal{X}_{V, T}^2 \simeq \mathcal{X}_{V^*, T}^2$ and observe that

$$|(\mu \mid v_n) - (\mu \mid v)|$$

$$= \left| \int_0^T \Big((\mu(t) \mid v_n(t)) - (\mu(t) \mid v(t)) \Big) \, dt \right|$$

$$= \left| \int_0^T \Big(\big(\mu(t) \mid (L_{\varphi_{j_n}(t)}^{-1} - L_{\varphi_j(t)}^{-1}) j_n(t) \big) + \big(\mu(t) \mid L_{\varphi_j(t)}^{-1} (j_n(t) - j(t)) \big) \Big) \, dt \right|$$

$$\leq \int_0^T \|\mu(t)\|_{V^*} \|L_{\varphi_{j_n}(t)}^{-1} - L_{\varphi_j(t)}^{-1}\|_{\mathscr{L}(V^*, V)} \|j_n(t)\|_{V^*} \, dt$$

$$+ \left| \int_0^T \big(\mu(t) \mid L_{\varphi_j(t)}^{-1} (j_n(t) - j(t)) \big) \, dt \right|.$$

Lemma 2(iv), the Lipschitz condition on $\varphi \mapsto A_\varphi$, and Lemma 5 imply

$$\begin{aligned}
\|L_{\varphi_{j_n}(t)}^{-1} - L_{\varphi_j(t)}^{-1}\|_{\mathscr{L}(V^*, V)} &\leq \frac{1}{\omega^2} \|A_{\varphi_{j_n}(t)} - A_{\varphi_j(t)}\|_{\mathscr{L}(V, V^*)} \\
&\leq \frac{\ell_A}{\omega^2} \|\varphi_{j_n}(t) - \varphi_j(t)\|_{1,\infty}^{M_0} \to 0.
\end{aligned} \tag{26}$$

In addition, note that $j' \mapsto \int_0^T (\mu(t) \mid L_{\varphi_j(t)}^{-1} j'(t)) \, dt$ is a bounded linear functional on $\mathcal{X}_{V^*, T}^2$. We conclude that $|(\mu \mid v_n) - (\mu \mid v)| \to 0$ by the dominated convergence theorem and $j_n \rightharpoonup j$ in $\mathcal{X}_{V^*, T}^2$.

Now we show that

$$\int_0^T (j(t)\,|\,v(t))\,dt \le \liminf_{n\to\infty} \int_0^T (j_n(t)\,|\,v_n(t))\,dt.$$

The mapping $v' \mapsto \int_0^T (L_{\varphi_j}(t)\,v'(t)\,|\,v'(t))\,dt$ is strongly continuous and convex on $\mathcal{X}^2_{V,T}$ since

$$\begin{aligned}
\|L_{\varphi_j(t)}\|_{\mathscr{L}(V,V^*)} &= \|\omega K_V^{-1} + A_{\varphi_j(t)}\|_{\mathscr{L}(V,V^*)} \\
&\le \omega + \|A_{id}\|_{\mathscr{L}(V,V^*)} + \ell_A \|\varphi_{j_n}(t) - \varphi_j(t)\|_{1,\infty}^{M_0} \le C_J
\end{aligned}$$

and $(L_{\varphi_j(t)}\,v''\,|\,v'') = \omega\,\|v''\|_V^2 + (A_{\varphi_j(t)}\,v''\,|\,v'') \ge 0$.

The mapping is therefore weakly lower semicontinuous. We then have

$$\begin{aligned}
&\liminf_{n\to\infty} \int_0^T (j_n(t)\,|\,v_n(t))\,dt \\
&= \liminf_{n\to\infty} \int_0^T \left(\omega\,\|v_n(t)\|_V^2 + (A_{\varphi_{j_n}(t)}\,v_n(t)\,|\,v_n(t))\right)\,dt \\
&= \liminf_{n\to\infty} \int_0^T \left((L_{\varphi_j}(t)\,v_n(t)\,|\,v_n(t)) + ((A_{\varphi_{j_n}(t)} - A_{\varphi_j(t)})\,v_n(t)\,|\,v_n(t))\right)\,dt \\
&\ge \int_0^T (L_{\varphi_j}(t)\,v(t)\,|\,v(t))\,dt = \int_0^T (j(t)\,|\,v(t))\,dt,
\end{aligned}$$

where the second to last inequality follows from $v_n \rightharpoonup v$, the weak lower semicontinuity of $v' \mapsto \int_0^T (L_{\varphi_j}(t)\,v'(t)\,|\,v'(t))\,dt$, the inequality $\|v_n\|_{\mathcal{X}^2_{V,T}} \le \frac{J}{\omega}$, and $\|A_{\varphi_{j_n}(t)} - A_{\varphi_j(t)}\|_{\mathscr{L}(V,V^*)} \to 0$ by (26). $\qquad\square$

6.5. **Proof of Theorem 2(ii).** The analysis is similar. It suffices to show that for a convergent sequence $\theta_n \to \theta$ in Θ, one has $\|\varphi_{\theta_n}(T) - \varphi_\theta(T)\|_{1,\infty}^{M_0} \to 0$, where φ_{θ_n} and φ_θ are the solutions to system (4) corresponding to θ_n and θ.

For all $\varphi \in C([0,T], Diff_{id}^1(\mathbb{R}^3))$ and $\theta' \in \Theta$, the boundedness assumption on $j(\cdot, \theta')$ gives $\int_0^T \|j(\varphi(t), \theta')\|_{V^*}\,dt \le J_\Theta\,T$, so Lemma 3 implies $(\varphi_{\theta_n})_{n=1}^\infty \subset \mathfrak{S}_{B_\Theta}$ and $\varphi_\theta \in \mathfrak{S}_{B_\Theta}$, where

$$B_\Theta = \frac{2c_V}{\omega}\,(J_\Theta\,T)\,\exp\left(\frac{c_V}{\omega}(J_\Theta\,T)\right).$$

We denote the Lipschitz constants of $\varphi \mapsto A_\varphi$ and $\{j(\cdot, \theta) : \theta \in \Theta\}$ on $\mathfrak{S}_{B_\Theta}$ by ℓ_A and ℓ_j respectively.

Observe that

$$
\begin{aligned}
&\varphi_{\theta_n}(t, x) - \varphi_\theta(t, x) \\
&= \int_0^t \left(v_{\varphi_{\theta_n}(s), j(\varphi_{\theta_n}(s), \theta_n)} \circ \varphi_{\theta_n}(s, x) - v_{\varphi_\theta(s), j(\varphi_\theta(s), \theta)} \circ \varphi_\theta(s, x) \right) ds \\
&= \int_0^t \left(\left(L_{\varphi_{\theta_n}(s)}^{-1} j(\varphi_{\theta_n}(s), \theta_n) \right) \circ \varphi_{\theta_n}(s, x) - \left(L_{\varphi_\theta(s)}^{-1} j(\varphi_{\theta_n}(s), \theta_n) \right) \circ \varphi_{\theta_n}(s, x) \right) ds \\
&\quad + \int_0^t \left(\left(L_{\varphi_\theta(s)}^{-1} j(\varphi_{\theta_n}(s), \theta_n) \right) \circ \varphi_{\theta_n}(s, x) - \left(L_{\varphi_\theta(s)}^{-1} j(\varphi_{\theta_n}(s), \theta_n) \right) \circ \varphi_\theta(s, x) \right) ds \\
&\quad + \int_0^t \left(\left(L_{\varphi_\theta(s)}^{-1} j(\varphi_{\theta_n}(s), \theta_n) \right) \circ \varphi_\theta(s, x) - \left(L_{\varphi_\theta(s)}^{-1} j(\varphi_\theta(s), \theta_n) \right) \circ \varphi_\theta(s, x) \right) ds \\
&\quad + \int_0^t \left(\left(L_{\varphi_\theta(s)}^{-1} j(\varphi_\theta(s), \theta_n) \right) \circ \varphi_\theta(s, x) - \left(L_{\varphi_\theta(s)}^{-1} j(\varphi_\theta(s), \theta) \right) \circ \varphi_\theta(s, x) \right) ds \\
&=: I_{1,n}(t) + I_{2,n}(t) + I_{3,n}(t) + \Lambda_n(t)
\end{aligned}
$$

With the same reasoning as in the proof of Theorem 1(ii), we bound $\|I_{1,n}(t)\|_{1,\infty}^{M_0}$ (see (21)) by

$$
\begin{aligned}
&\|I_{1,n}(t)\|_{1,\infty}^{M_0} \\
&\leq \frac{c_V}{\omega^2} (2 + B_\Theta) \ell_A \int_0^t \|\varphi_{\theta_n}(s) - \varphi_\theta(s)\|_{1,\infty}^{M_0} \|j(\varphi_{\theta_n}(s), \theta_n)\|_{V^*} ds \\
&\leq C_\Theta \int_0^t \|\varphi_{\theta_n}(s) - \varphi_\theta(s)\|_{1,\infty}^{M_0} ds,
\end{aligned}
$$

and $\|I_{2,n}(t)\|_{1,\infty}^{M_0}$ (see (22)) by

$$
\begin{aligned}
&\|I_{2,n}(t)\|_{1,\infty}^{M_0} \\
&\leq \frac{c_V}{\omega} (2 + B_\Theta) \int_0^t \|j(\varphi_{\theta_n}(s), \theta_n)\|_{V^*} \|\varphi_{\theta_n}(s) - \varphi_\theta(s)\|_{1,\infty}^{M_0} ds \\
&\leq C_\Theta \int_0^t \|\varphi_{\theta_n}(s) - \varphi_\theta(s)\|_{1,\infty}^{M_0} ds.
\end{aligned}
$$

The assumption that $\{j(\cdot, \theta) : \theta \in \Theta\}$ is equi-Lipschitz with respect to $\|\cdot\|_{1,\infty}^{M_0}$ gives the following estimate of $\|I_{3,n}(t)\|_{1,\infty}^{M_0}$:

$$\|I_{3,n}(t)\|_{1,\infty}^{M_0}$$

$$= \left\| \int_0^t \left(\left(L_{\varphi_\theta(s)}^{-1} j(\varphi_{\theta_n}(s), \theta_n) \right) \circ \varphi_\theta(s) - \left(L_{\varphi_\theta(s)}^{-1} j(\varphi_\theta(s), \theta_n) \right) \circ \varphi_\theta(s) \right) ds \right\|_{1,\infty}^{M_0}$$

$$\leq \int_0^t \left\| \left(L_{\varphi_\theta(s)}^{-1} j(\varphi_{\theta_n}(s), \theta_n) \right) \circ \varphi_\theta(s) - \left(L_{\varphi_\theta(s)}^{-1} j(\varphi_\theta(s), \theta_n) \right) \circ \varphi_\theta(s) \right\|_{1,\infty} ds$$

$$\leq \int_0^t (2 + \|\varphi_\theta(s) - id\|_{1,\infty}) \left\| L_{\varphi_\theta(s)}^{-1} j(\varphi_{\theta_n}(s), \theta_n) - L_{\varphi_\theta(s)}^{-1} j(\varphi_\theta(s), \theta_n) \right\|_{1,\infty} ds$$

$$\leq (2 + B_\Theta) \frac{c_V}{\omega} \ell_j \int_0^t \|\varphi_{\theta_n}(s) - \varphi_\theta(s)\|_{1,\infty}^{M_0} ds$$

$$= C_\Theta \int_0^t \|\varphi_{\theta_n}(s) - \varphi_\theta(s)\|_{1,\infty}^{M_0} ds.$$

We now work on $\|\Lambda_n(t)\|_{1,\infty}^{M_0}$. Recall that

$$\Lambda_n(t) = \int_0^t \left(\left(L_{\varphi_\theta(s)}^{-1} j(\varphi_\theta(s), \theta_n) \right) \circ \varphi_\theta(s) - \left(L_{\varphi_\theta(s)}^{-1} j(\varphi_\theta(s), \theta) \right) \circ \varphi_\theta(s) \right) ds.$$

To carry over the last set of arguments in the proof of Theorem 1(ii), it remains to show that $\lim_{n\to\infty} \|\Lambda_n(t)\|_{1,\infty}^{M_0} = 0$ for each $t \in [0, T]$ and $\|\Lambda_n(t)\|_{1,\infty}^{M_0}$ is uniformly bounded in n and t. Following inequality (25), the uniform boundedness of $\|\Lambda_n(t)\|_{1,\infty}^{M_0}$ in n and t is given by

$$\|\Lambda_n(t)\|_{1,\infty}^{M_0} \leq \int_0^t (2 + B_\Theta) \frac{c_V}{\omega} \left(\|j(\varphi_\theta(s), \theta_n)\|_{V^*} + \|j(\varphi_\theta(s), \theta)\|_{V^*} \right) ds \leq C_\Theta.$$

To prove $\lim_{n\to\infty} \|\Lambda_n(t)\|_{1,\infty}^{M_0} = 0$ for each t, we define the integrands of the two terms in $\Lambda_n(t)$ as $u_n : [0, T] \times \mathbb{R}^3 \to \mathbb{R}^3$ and $u : [0, T] \times \mathbb{R}^3 \to \mathbb{R}^3$ by

$$u_n(s, x) = \left(L_{\varphi_\theta(s)}^{-1} j(\varphi_\theta(s), \theta_n) \right) \circ \varphi_\theta(s, x)$$

and

$$u(s, x) = \left(L_{\varphi_\theta(s)}^{-1} j(\varphi_\theta(s), \theta) \right) \circ \varphi_\theta(s, x).$$

We show that the two sequences $(\int_0^t u_n(s)\, ds)_{n=1}^\infty$ and $(\int_0^t Du_n(s)\, ds)_{n=1}^\infty$ converge pointwise, are uniformly bounded, and are equicontinuous. Given $s \in [0, T]$ and $x \in \mathbb{R}^3$, define linear operators $\mathcal{L}_{s,x} : V^* \to \mathbb{R}^3$ and $\widetilde{\mathcal{L}}_{s,x} : V^* \to \mathbb{R}^{3\times 3}$ by

$$\mathcal{L}_{s,x} j' = \left(L_{\varphi_\theta(s)}^{-1} j' \right) \circ \varphi_\theta(s, x) \quad \text{and} \quad \widetilde{\mathcal{L}}_{s,x} j' = D\left(L_{\varphi_\theta(s)}^{-1} j' \circ \varphi_\theta(s, x) \right),$$

which can be estimated by

$$|\mathcal{L}_{s,x} j'| + |\widetilde{\mathcal{L}}_{s,x} j'| \leq \left\| \left(L_{\varphi_\theta(s)}^{-1} j' \right) \circ \varphi_\theta(s) \right\|_{1,\infty} \leq \frac{c_V}{\omega} (2 + B_\Theta) \|j'\|_{V^*}, \tag{27}$$

so both $\mathcal{L}_{s,x}$ and $\widetilde{\mathcal{L}}_{s,x}$ are bounded linear operators for all $s \in [0, T]$ and $x \in \mathbb{R}^3$. Since $j(\varphi_\theta(s), \theta_n) \rightharpoonup j(\varphi_\theta(s), \theta)$ when $\theta_n \to \theta$, we obtain pointwise convergence of $(u_n(s))_{n=1}^\infty$ and $(Du_n(s))_{n=1}^\infty$ for each $s \in [0, T]$. Uniform boundedness and pointwise convergence of

$(\int_0^t u_n(s)\, ds)_{n=1}^\infty$ and $(\int_0^t Du_n(s)\, ds)_{n=1}^\infty$ follow from inequality (27), $\int_0^T \|j(\varphi_\theta(s), \theta_n)\|_{V^*}\, ds \leq J_\Theta T$, and the dominated convergence theorem. The same process as the one in the proof of Theorem 1(ii) shows equicontinuity under different constants. Invoking the Arzelà–Ascoli theorem gives us $\lim_{n\to\infty} \| \int_0^t (u_n(s) - u(s))\, ds\|_\infty^{M_0} = 0$ and $\lim_{n\to\infty} \| \int_0^t (Du_n(s) - Du(s))\, ds\|_\infty^{M_0} = 0$, which in turn implies $\|\Lambda_n(t)\|_{1,\infty}^{M_0} \to 0$ for each $t \in [0, T]$.

We have thus proved that

$$\|\varphi_{\theta_n}(t) - \varphi_\theta(t)\|_{1,\infty}^{M_0} \leq \|\Lambda_n(t)\|_{1,\infty}^{M_0} + C_\Theta \int_0^t \|\varphi_{\theta_n}(s) - \varphi_\theta(s)\|_{1,\infty}^{M_0}\, ds,$$

where $\lim_{n\to\infty} \|\Lambda_n(t)\|_{1,\infty}^{M_0} = 0$ for each $t \in [0, T]$ and $\|\Lambda_n(t)\|_{1,\infty}^{M_0}$ is uniformly bounded in n and t. Applying Gronwall's lemma and the dominated convergence theorem as in the proof of Theorem 1(ii), we conclude that for each $t \in [0, T]$,

$$\|\varphi_{\theta_n}(t) - \varphi_\theta(t)\|_{1,\infty}^{M_0} \to 0 \ \text{ as } \ n \to \infty.$$

6.6. **Proof of Proposition 1.** We need to check that: (1) $A_\varphi \in \mathscr{L}_{\mathrm{sym}}(V, V^*)$ for all $\varphi \in \mathit{Diff}_{id}^1(\mathbb{R}^3)$; (2) $(A_\varphi v \,|\, v) \geq 0$ for all $\varphi \in \mathit{Diff}_{id}^1(\mathbb{R}^3)$ and $v \in V$; (3) The mapping $\varphi \mapsto A_\varphi$ is Lipschitz with respect to $\|\cdot\|_{1,\infty}^{M_0}$ on $\mathfrak{S}_\gamma$. Point (2) is obvious from the assumption that $E_\varphi(x)$ is positive definite for all $x \in \varphi(M_0)$. Since $id \in \mathfrak{S}_\gamma$ for all $\gamma > 0$, we can derive point (1) from the inequality

$$|(A_\varphi u \,|\, v)| \leq \int_{M_0} \left| \left(E_\varphi(\varepsilon_u, \varepsilon_v) \right) \circ \varphi \,|\det D\varphi| \right| dx$$

$$\leq \|Du\|_\infty \|Dv\|_\infty \|\det D\varphi\|_\infty \left(\int_{M_0} |E_{id} \circ id|\, dx + C_\varphi \right)$$

$$\leq (c_V^2\, C_\varphi)\, \|u\|_V \|v\|_V.$$

We now proceed to proving point (3). For $\varphi, \psi \in \mathfrak{S}_\gamma$, we show that there exists C_γ such that

$$|(A_\varphi u \,|\, v) - (A_\psi u \,|\, v)| \leq C_\gamma \|\varphi - \psi\|_{1,\infty}^{M_0} \|u\|_V \|v\|_V.$$

We make a change of variables and write

$$
\begin{aligned}
&|(A_\varphi u \,|\, v) - (A_\psi u \,|\, v)| \\
&\leq \int_{M_0} \left| \left(E_\varphi(\varepsilon_u, \varepsilon_v) \right) \circ \varphi \,|\det D\varphi| - \left(E_\psi(\varepsilon_u, \varepsilon_v) \right) \circ \psi \,|\det D\psi| \right| dx \\
&\leq \int_{M_0} \left| (E_\varphi \circ \varphi - E_\psi \circ \psi)(\varepsilon_u \circ \varphi, \varepsilon_v \circ \varphi) \right| |\det D\varphi|\, dx \\
&\quad + \int_{M_0} \left| (E_\psi \circ \psi)(\varepsilon_u \circ \varphi - \varepsilon_u \circ \psi, \varepsilon_v \circ \varphi) \right| |\det D\varphi|\, dx \\
&\quad + \int_{M_0} \left| (E_\psi \circ \psi)(\varepsilon_u \circ \psi, \varepsilon_v \circ \varphi - \varepsilon_v \circ \psi) \right| |\det D\varphi|\, dx \\
&\quad + \int_{M_0} \left| (E_\psi \circ \psi)(\varepsilon_u \circ \psi, \varepsilon_v \circ \psi) \right| \left| |\det D\varphi| - |\det D\psi| \right| dx.
\end{aligned}
\tag{28}
$$

For the first term in (28), the assumption on E yields

$$\int_{M_0} \left|(E_\varphi \circ \varphi - E_\psi \circ \psi)(\varepsilon_u \circ \varphi, \, \varepsilon_v \circ \varphi)\right| |\det D\varphi| \, dx$$

$$\leq \|Du\|_\infty \|Dv\|_\infty \|\det D\varphi\|_\infty \int_{M_0} \left|(E_\varphi \circ \varphi - E_\psi \circ \psi)\right| dx \tag{29}$$

$$\leq C_\gamma \|\varphi - \psi\|_{1,\infty}^{M_0} \|u\|_V \|v\|_V,$$

where we have used $\|\det D\varphi\|_\infty \leq C_\gamma$ for all $\varphi \in \mathfrak{S}_\gamma$.

We estimate the second and third terms together by symmetry. Again note that $id \in \mathfrak{S}_\gamma$ for all $\gamma > 0$, so

$$\int_{M_0} |E_\psi \circ \psi| \, dx \leq \int_{M_0} |E_{id} \circ id| \, dx + \alpha_\gamma \|\psi - id\|_{1,\infty}^{M_0} \leq \int_{M_0} |E_{id}| \, dx + \alpha_\gamma \, \gamma = C_\gamma.$$

It follows that

$$\int_{M_0} \left|(E_\psi \circ \psi)(\varepsilon_u \circ \varphi - \varepsilon_u \circ \psi, \, \varepsilon_v \circ \varphi)\right| |\det D\varphi| \, dx$$

$$+ \int_{M_0} \left|(E_\psi \circ \psi)(\varepsilon_u \circ \psi, \, \varepsilon_v \circ \varphi - \varepsilon_v \circ \psi)\right| |\det D\varphi| \, dx$$

$$\leq \|D^2 u\|_\infty \|\varphi - \psi\|_\infty^{M_0} \|Dv\|_\infty \|\det D\varphi\|_\infty \int_{M_0} |E_\psi \circ \psi| \, dx \tag{30}$$

$$+ \|Du\|_\infty \|D^2 v\|_\infty \|\varphi - \psi\|_\infty^{M_0} \|\det D\varphi\|_\infty \int_{M_0} |E_\psi \circ \psi| \, dx$$

$$\leq C_\gamma \|\varphi - \psi\|_{1,\infty}^{M_0} \|u\|_V \|v\|_V.$$

For the fourth term, we use inequality (10) and write

$$\int_{M_0} \left|(E_\psi \circ \psi)(\varepsilon_u \circ \psi, \, \varepsilon_v \circ \psi)\right| \left||\det D\varphi| - |\det D\psi|\right| dx$$

$$\leq C \left(\|D\varphi\|_\infty + \|D\psi\|_\infty\right)^2 \|D\varphi - D\psi\|_\infty^{M_0} \|Du\|_\infty \|Dv\|_\infty \int_{M_0} |E_\psi \circ \psi| \, dx \tag{31}$$

$$\leq C_\gamma \|\varphi - \psi\|_{1,\infty}^{M_0} \|u\|_V \|v\|_V.$$

Combining inequality (28) with estimates (29)–(31), we conclude that

$$|(A_\varphi u \,|\, v) - (A_\psi u \,|\, v)| \leq C_\gamma \|\varphi - \psi\|_{1,\infty}^{M_0} \|u\|_V \|v\|_V.$$

To justify that the operator in equation (11) also satisfies the hypotheses, we note that the penalty term can be rewritten as

$$\beta \int_{\mathcal{M}_{\text{bottom}}} ((u \circ \varphi)^\top D\varphi^{-\top} n_0)((w \circ \varphi)^\top D\varphi^{-\top} n_0) \frac{|\det D\varphi|}{|D\varphi^{-\top} n_0|} \, d\sigma$$

(where n_0 is a unit normal to $\mathcal{M}_{\text{bottom}}$). One can then work on the terms in the integral using similar arguments to those made in the previous proof.

7. Conclusion

In this paper, we first examined the existence and uniqueness of solutions to general systems $\partial_t \varphi(t,x) = v(t, \varphi(t,x))$, $\varphi(0,x) = x$, where the vector field is a function of a yank j of the form $v(t) = L_{\varphi(t)}^{-1} j(t)$ or $v(t) = L_{\varphi(t)}^{-1} j(\varphi(t), \theta)$. We then extended the analysis to prove the existence of solutions to the corresponding inverse problems in which one attempts to recover the yank or the parameters from the observed initial and final volumes.

Although we have focused on the specific operator $L_\varphi^{-1} = (\omega K_V^{-1} + A_\varphi)^{-1} \in \mathcal{L}(V^*, V)$, our theorems can be generalized to an operator in $\mathcal{L}(V^*, V)$ satisfying similar conditions of boundedness and regularity.

We have presented results of simulated inverse problems assuming shapes are hyperelastic materials. Our results indicate that the elasticity assumption together with the data from the boundary of target are not enough to determine the internal yank. Additional information such as the internal structure of the target or a parametric model for j is necessary to tackle these inverse problems. As a proof of concept, we have considered a simple form of yank whose density is the gradient of a parametrized potential advected by deformation and demonstrated the retrievability of the potential function parameters under this setting. A more sophisticated model should likely involve propagation of the potential in addition to advection as a way to account for, e.g., the progression of pathology along with morphological changes. A possible approach could be to combine the shape evolution equations discussed in this paper with, for example, a reaction-diffusion PDE on the potential function to model its dynamics. We are currently investigating a model of this kind, which comes with the extra technicality of dealing with such PDEs on varying domains, and hope to publish relevant results in the near future.

Appendix A. Implementation details

Appendix A.1 covers discretization specific to templates with layered structures. (One may use any discretization procedure if layered structures are not of concern.) In Appendix A.2, we include the computation of the gradient of the parametric yank problem with the elastic operators and yank presented in section 4. The computation of the gradient of the free yank problem can be adapted from Appendix A.2.

A.1. **Tetrahedralization of layered templates.** We use the notation of Example 3. The template shape M_0 is discretized into a set of points $\bigcup_{\ell=1}^{L} \{q_i^\ell\}_{i=1}^{N}$ according to its layered structure Φ. Points $\{q_i^\ell\}_{i=1}^{N}$ are on the same layer ν_ℓ, and the vectors $q_i^{\ell+1} - q_i^\ell$ are parallel to the transversal vector $\partial_\nu \Phi(q_i^1, \nu_\ell)$ at q_i^ℓ for all i and ℓ (Figures 11a and 11b). Note that points $\{q_i^1\}_{i=1}^{N}$ are on the bottom layer, points $\{q_i^L\}_{i=1}^{N}$ are on the top layer, and each discretized layer has the same number of discretized points. Since Φ is a diffeomorphism, the same triangulation structure can be applied to each layer (Figure 11c). It follows that $\{q_{i_1}^\ell, q_{i_2}^\ell, q_{i_3}^\ell, q_{i_1}^{\ell+1}, q_{i_2}^{\ell+1}, q_{i_3}^{\ell+1}\}$ forms a triangular prism for any triangular face (i_1, i_2, i_3) of one layer. Those prisms between the first and second layers are further split into tetrahedra without adding vertices using the procedure introduced in [14], which guarantees consistent triangular faces across adjacent prisms. To ensure the same tetrahedralization structure between consecutive layers, the tetrahedralization between the first and second layers is then replicated to prisms between consecutive upper layers (Figure 11d).
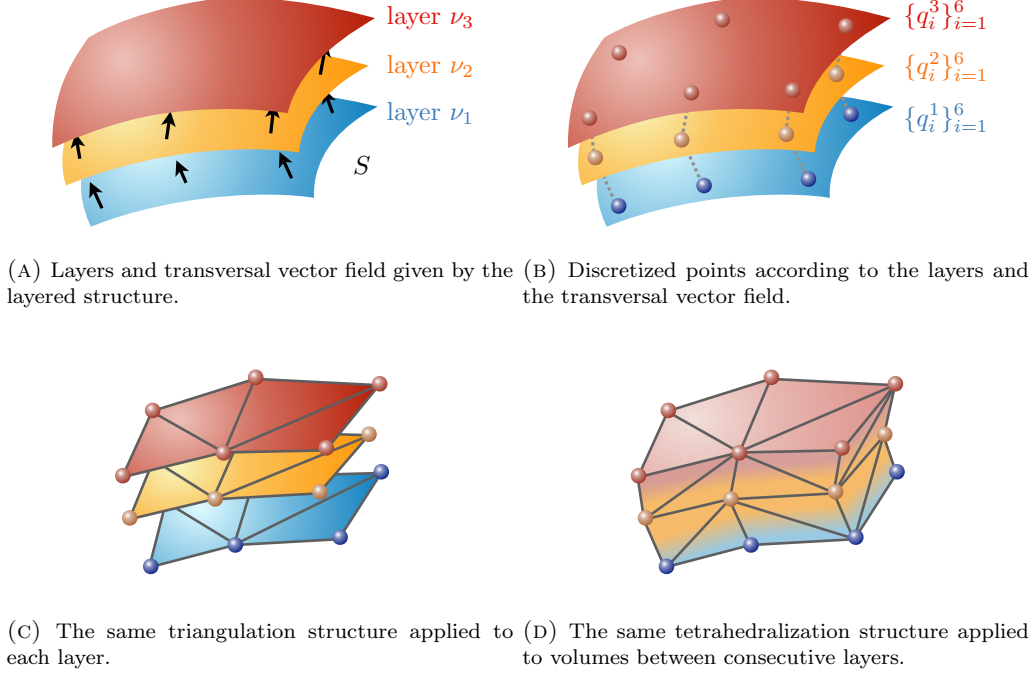
(A) Layers and transversal vector field given by the layered structure.

(B) Discretized points according to the layers and the transversal vector field.

(C) The same triangulation structure applied to each layer.

(D) The same tetrahedralization structure applied to volumes between consecutive layers.

FIGURE 11. Tetrahedralization of layered templates.

A.2. **Gradient computation.** We write down the gradient of our optimization problem assuming a continuous time variable, which can be easily discretized in time once an integration scheme for ODEs is selected. Denote the discretized M_0 by $q_0 \in \mathbb{R}^{3n}$ and the discretized M_{targ} by $q_{\mathrm{targ}} \in \mathbb{R}^{3n'}$ ($n = NL$ for layered templates). Moreover, denote the kernel matrix of the RKHS V by $\boldsymbol{K}_q \in \mathbb{R}^{3n \times 3n}$, namely for $q = (q_i)_{i=1,\ldots,n}$, $\boldsymbol{K}_q = (K(q_i, q_j))_{i,j=1,\ldots,n}$ where $K : \mathbb{R}^3 \times \mathbb{R}^3 \to \mathbb{R}^{3 \times 3}$ is the kernel function associated to the vector RKHS V. Finally, we write the discretized operator $(A_\varphi u \mid w)$ as $u^\top \boldsymbol{A}_q w$, and the discretized work $(j(\varphi, \theta) \mid w)$ as $j_{q,\theta}^\top w$. It follows that the optimal velocity expressed in Lemma 1 becomes $v_{q,\theta} = (\omega \boldsymbol{K}_q^{-1} + \boldsymbol{A}_q)^{-1} j_{q,\theta} =: \boldsymbol{L}_q^{-1} j_{q,\theta}$ and is obtained numerically by solving a $3n$-by-$3n$ symmetric positive-definite linear system. The discretized optimization problem now becomes

$$\min_{\theta \in \Theta} \ \rho(q(T), q_{\mathrm{targ}})$$

subject to $\dot{q}(t) = v_{q(t), \theta}$ and $q(0) = q_0$. Introduce the costate $p(\cdot)$, where $p(t) \in \mathbb{R}^{3n}$. We then form the Lagrangian

$$\mathcal{L}(q, p, \theta) = \rho(q(T), q_{\mathrm{targ}}) + \int_0^T p(t)^\top (\dot{q}(t) - v_{q(t), \theta}) \, dt.$$

For each θ, we look for q_θ and p_θ such that

$$\begin{cases} \dot{q}_\theta(t) = v_{q_\theta(t),\,\theta}, \ q_\theta(0) = q_0, \\ D_q\mathcal{L}(q_\theta, p_\theta, \theta) = 0, \\ D_p\mathcal{L}(q_\theta, p_\theta, \theta) = 0. \end{cases}$$

With such chosen q_θ and p_θ, we deduce that $\partial_{\theta'}\mathcal{L}(q_\theta, p_\theta, \theta')|_{\theta'=\theta}$ is the gradient of our discretized optimization problem. We now show how to obtain q_θ and p_θ. Derivatives of $\mathcal{L}$ with respect to q and p are given by

$$\begin{cases} (D_q\mathcal{L}(q,p,\theta)\,|\,\delta q) = \left(\partial_{q(T)}\rho(q(T), q_{\mathrm{targ}})\right)^\top \delta q(T) + p(T)^\top \delta q(T) \\ \qquad\qquad\qquad\qquad - \displaystyle\int_0^T \left(\dot{p}(t) + \partial_{q(t)}(p(t)^\top v_{q(t),\,\theta})\right)^\top \delta q(t)\,dt, \\ (D_p\mathcal{L}(q,p,\theta)\,|\,\delta p) = \displaystyle\int_0^T \delta p(t)^\top \left(\dot{q}(t) - v_{q(t),\,\theta}\right) dt\,. \end{cases}$$

Note that $D_q\mathcal{L}(q,p,\theta) = 0$ is equivalent to $\dot{p}(t) = -\partial_{q(t)}(p(t)^\top v_{q(t),\,\theta})$ and $p(T) = -\partial_{q(T)}\rho(q(T), q_{\mathrm{targ}})$. In addition, $D_p\mathcal{L}(q,p,\theta) = 0$ is equivalent to $\dot{q}(t) = v_{q(t),\,\theta}$. Hence we can compute the gradient as follows. First we compute q_θ as a solution of

$$\dot{q}(t) = v_{q(t),\,\theta}, \ q(0) = q_0.$$

Plugging q_θ into the ODE of p, next we solve

$$\dot{p}(t) = -\partial_{q(t)}(p(t)^\top v_{q_\theta(t),\,\theta}), \ p(T) = -\partial_{q(T)}\rho(q_\theta(T), q_{\mathrm{targ}})$$

for p_θ. Since q_θ and p_θ satisfy the requirements, we can compute the gradient of our discretized optimization problem as

$$\partial_{\theta'}\mathcal{L}(q_\theta, p_\theta, \theta')|_{\theta'=\theta} = -\int_0^T \partial_{\theta'}(p_\theta(t)^\top v_{q_\theta(t),\,\theta'})\big|_{\theta'=\theta}\,dt.$$

Now the computation of gradient is broken down into three terms: $\partial_q(p^\top v_{q,\theta})$, $\partial_{q(T)}\rho(q(T), q_{\mathrm{targ}})$, and $\partial_\theta(p^\top v_{q,\theta})$. We will use the notation $u_q^\top (\partial_q \boldsymbol{A}_q)\,w_q$ in the following to mean the differentiation of $u_q^\top \boldsymbol{A}_q\,w_q$ with respect to q while keeping u_q and w_q fixed. Similarly, the notation $(\partial_q j_{q,\theta})^\top w_q$ means the differentiation of $j_{q,\theta}^\top w_q$ with respect to q when we fix w_q. With those conventions set, we can now formally compute

$$\begin{aligned} \partial_q(p^\top v_{q,\theta}) &= \partial_q\left(p^\top \boldsymbol{L}_q^{-1} j_{q,\theta}\right) \\ &= -(\boldsymbol{L}_q^{-1}p)^\top (\partial_q \boldsymbol{L}_q)\,(\boldsymbol{L}_q^{-1} j_{q,\theta}) + (\boldsymbol{L}_q^{-1}p)^\top (\partial_q j_{q,\theta}) \\ &= -(\boldsymbol{L}_q^{-1}p)^\top (\omega\,\partial_q \boldsymbol{K}_q^{-1} + \partial_q \boldsymbol{A}_q)\,(\boldsymbol{L}_q^{-1} j_{q,\theta}) + (\boldsymbol{L}_q^{-1}p)^\top (\partial_q j_{q,\theta}) \\ &= \omega\,(\boldsymbol{K}_q^{-1}\beta_{q,p})^\top (\partial_q \boldsymbol{K}_q)\,(\boldsymbol{K}_q^{-1} v_{q,\theta}) - \beta_{q,p}^\top (\partial_q \boldsymbol{A}_q)\,v_{q,\theta} + \beta_{q,p}^\top (\partial_q j_{q,\theta}), \end{aligned}$$

where $\beta_{q,p} = \boldsymbol{L}_q^{-1}p$.

We present computations of $u^\top \boldsymbol{A}_q\,w$ in Appendix A.2.1, $\boldsymbol{A}_q\,w$ in Appendix A.2.2, $u^\top (\partial_q \boldsymbol{A}_q)\,w$ in Appendix A.2.3, $j_{q,\theta}^\top w$ in Appendix A.2.4, $j_{q,\theta}$ in Appendix A.2.5, and $(\partial_q j_{q,\theta})^\top w$ in Appendix A.2.6, which are essential in the above computation of $\partial_q(p^\top v_{q,\theta})$. The computation of $\partial_{q(T)}\rho(q(T), q_{\mathrm{targ}})$ depends on the discrepancy function ρ. We refer to [11] when ρ is the varifold discrepancy between triangulated surfaces. Since

$$\partial_\theta(p^\top v_{q,\theta}) = \partial_\theta(p^\top \boldsymbol{L}_q^{-1} j_{q,\theta}) = \partial_\theta(\beta_{q,p}^\top j_{q,\theta}),$$

the computation of $\partial_\theta(p^\top v_{q,\theta})$ can be derived from $j_{q,\theta}^\top w$ (Appendix A.2.4).

To make the presentation more concrete, we focus on the layered elastic operator and yank described in section 4.

A.2.1. *Computation of $\boldsymbol{u}^\top \boldsymbol{A_q}\, \boldsymbol{w}$*. A little computation shows that the layered elastic operator (9) can be rewritten as

$$
\begin{aligned}
(A_\varphi u \mid w) = \int_{\varphi(M_0)} & \left(\lambda_{\text{tan}} \left(\text{tr}(\varepsilon_u) - N_\varphi^\top \varepsilon_u N_\varphi \right) \left(\text{tr}(\varepsilon_w) - N_\varphi^\top \varepsilon_w N_\varphi \right) \right. \\
& + \mu_{\text{tan}} \left(\text{tr}(\varepsilon_u \varepsilon_w) - 2\, N_\varphi^\top \varepsilon_u \varepsilon_w N_\varphi + (N_\varphi^\top \varepsilon_u N_\varphi)(N_\varphi^\top \varepsilon_w N_\varphi) \right) \\
& + \mu_{\text{tsv}} \, (S_\varphi^\top \varepsilon_u S_\varphi)(S_\varphi^\top \varepsilon_w S_\varphi) \\
& \left. + 2\,\mu_{\text{ang}} \left(S_\varphi^\top \varepsilon_u \varepsilon_w S_\varphi - (N_\varphi^\top \varepsilon_u S_\varphi)(N_\varphi^\top \varepsilon_w S_\varphi) \right) \right) dx,
\end{aligned}
\tag{32}
$$

where $\varepsilon_u = \frac{1}{2}\left(Du + Du^\top\right)$ and $\varepsilon_w = \frac{1}{2}\left(Dw + Dw^\top\right)$ are linear strain tensors, N_φ is a unit vector field normal to deformed layers $\{\varphi(\mathcal{M}_\nu) : \nu \in [0,1]\}$, and $S_\varphi = \frac{(D\varphi\,S)\circ\varphi^{-1}}{|(D\varphi\,S)\circ\varphi^{-1}|}$ is the unit transversal vector field according to the deformed layered structure. After discretizing $\varphi(M_0)$ into a union of tetrahedra, we compute the integral (32) by summing over these tetrahedra. Thus we can focus the computation on one single tetrahedron. Note that we need N_φ, S_φ, Du, and Dw to evaluate (32). Recall that the tetrahedralization procedure (Appendix A.1) splits one triangular prism into three tetrahedra. Given a tetrahedron, we compute N_φ as the average of normals of the two bases of the corresponding prism, and S_φ is computed as the average of three sides of the corresponding prism. To be more precise, let the "upward-pointing" unit normals of two bases be N_1 and N_2, and let the unit transversals from three sides be S_1, S_2, and S_3. The vectors N_φ and S_φ of the three tetrahedra split from this prism are computed by

$$
N_\varphi = \frac{N_1 + N_2}{|N_1 + N_2|} \quad \text{and} \quad S_\varphi = \frac{S_1 + S_2 + S_3}{|S_1 + S_2 + S_3|}.
$$

For the computation of Du, denote the positions at the four vertices of the tetrahedron by q_0, q_1, q_2, q_3, and denote u at the four vertices by u_0, u_1, u_2, u_3. We approximate $Du(q_0)$ by

$$
\begin{aligned}
Du(q_0) = Du(q_0) &\left[\; q_1 - q_0, \quad q_2 - q_0, \quad q_3 - q_0 \;\right] \left[\; q_1 - q_0, \quad q_2 - q_0, \quad q_3 - q_0 \;\right]^{-1} \\
&\approx \left[\; u_1 - u_0, \quad u_2 - u_0, \quad u_3 - u_0 \;\right] \left[\; q_1 - q_0, \quad q_2 - q_0, \quad q_3 - q_0 \;\right]^{-1}.
\end{aligned}
$$

The approximated $Du(q_0)$ within a tetrahedron $\mathcal{T}$, denoted by $(Du)_{\mathcal{T}}$, is characterized by

$$
\begin{cases}
(Du)_{\mathcal{T}}\,(q_1 - q_0) = u_1 - u_0 \\
(Du)_{\mathcal{T}}\,(q_2 - q_0) = u_2 - u_0 \\
(Du)_{\mathcal{T}}\,(q_3 - q_0) = u_3 - u_0
\end{cases},
$$

which is equivalent to

$$
\begin{cases}
(Du)_{\mathcal{T}}\,(q_0 - q_1) = u_0 - u_1 \\
(Du)_{\mathcal{T}}\,(q_2 - q_1) = u_2 - u_1 \\
(Du)_{\mathcal{T}}\,(q_3 - q_1) = u_3 - u_1
\end{cases}.
$$

The same pattern holds if we change the anchor position to q_2 and q_3. In other words, the approximated $(Du)_{\mathcal{T}}$ only depends on tetrahedron, not on the anchor position, the ordering

of vertices, or the choice of three edges from the tetrahedron. Dw is computed in exactly the same way.

A.2.2. *Computation of $\boldsymbol{A_q\,w} = \boldsymbol{\partial_u(u^\top A_q\,w)}$.* We use the same notation as in Appendix A.2.1 and keep focusing on one single tetrahedron. Note that we still denote the discretized ε_u by ε_u. Define

$$U = \left[\begin{array}{ccc} u_1 - u_0, & u_2 - u_0, & u_3 - u_0 \end{array}\right] \quad \text{and} \quad Q = \left[\begin{array}{ccc} q_1 - q_0, & q_2 - q_0, & q_3 - q_0 \end{array}\right],$$

so $(Du)_{\mathcal{T}} = UQ^{-1}$. Since $\operatorname{tr}(\varepsilon_u) = \sum_{i=1}^{3} e_i^\top \varepsilon_u\, e_i$, where e_i is the canonical basis of $\mathbb{R}^3$, we only need to have an expression of $\partial_{u_i}(a^\top \varepsilon_u\, b)$ for arbitrary $a, b \in \mathbb{R}^3$ in order to compute $\partial_u(u^\top A_q w)$ (see equation (32)). Note that

$$a^\top \varepsilon_u\, b = a^\top \left(\frac{1}{2} \left(UQ^{-1} + Q^{-\top} U^\top \right) \right) b = \frac{1}{2} \operatorname{tr}\!\left(Q^{-1}(ba^\top + ab^\top) U \right), \qquad (33)$$

which gives

$$\partial_{u_0}\!\left(a^\top \varepsilon_u\, b \right) = \left(-\frac{1}{2}\, \mathbb{1}_3^\top Q^{-1}(ba^\top + ab^\top) \right)^\top$$

and

$$\partial_{u_i}\!\left(a^\top \varepsilon_u\, b \right) = \left(\frac{1}{2}\, \left(Q^{-1}(ba^\top + ab^\top) \right)_{i*} \right)^\top \quad \text{for } i = 1, 2, 3,$$

where $\mathbb{1}_3$ denotes the 3-by-1 all-one vector, and $(A)_{i*}$ denotes the ith row of a matrix A.

Let k be the global index running through n discretized points. Note that when we compute $\partial_{u_k}(u^\top A_q w)$ by summing over tetrahedra, we only need to take into account those tetrahedra having q_k as a vertex. Other tetrahedra do not have u_k involved in our computation of $u^\top A_q w$. This information can be precomputed when we generate the tetrahedralization.

A.2.3. *Computation of $\boldsymbol{u^\top (\partial_q A_q)\,w} = \boldsymbol{\partial_q(u^\top A_q\,w)}$.* Differentiating N_φ, S_φ, and volume with respect to q is straightforward. Given a tetrahedron with q_0, q_1, q_2, q_3 as vertices, we look at $\partial_{q_i}(a^\top \varepsilon_u\, b)$ for arbitrary $a, b \in \mathbb{R}^3$. From (33), we deduce that

$$\partial_{q_0}\!\left(a^\top \varepsilon_u\, b \right) = \left(\frac{1}{2}\, \mathbb{1}_3^\top Q^{-1}(ba^\top + ab^\top) UQ^{-1} \right)^\top$$

and

$$\partial_{q_i}\!\left(a^\top \varepsilon_u\, b \right) = \left(-\frac{1}{2}\, \left(Q^{-1}(ba^\top + ab^\top) UQ^{-1} \right)_{i*} \right)^\top \quad \text{for } i = 1, 2, 3.$$

A.2.4. *Computation of $\boldsymbol{j_{q,\theta}^\top\, w}$.* Much of the work has been done in Appendices A.2.1 and A.2.2. Recall that

$$(j(\varphi, \theta) \mid w) = -\int_{\varphi(M_0)} \chi\; g_\theta \circ \varphi^{-1} \operatorname{div}(w)\, dx = -\int_{\varphi(M_0)} \chi\; g_\theta \circ \varphi^{-1} \operatorname{tr}(Dw)\, dx.$$

In a single transformed tetrahedron $\mathcal{T}$, we evaluate $\chi\, g_\theta \circ \varphi^{-1}$ at the transformed centroid to simplify the computation. Denote the evaluated value by $g_{\mathcal{T}}$. The derivative Dw is approximated in the same way as in Appendix A.2.1, that is, $(Dw)_{\mathcal{T}} = WQ^{-1}$, where

$$W = \left[\begin{array}{ccc} w_1 - w_0, & w_2 - w_0, & w_3 - w_0 \end{array}\right] \quad \text{and} \quad Q = \left[\begin{array}{ccc} q_1 - q_0, & q_2 - q_0, & q_3 - q_0 \end{array}\right].$$

The contribution of a single tetrahedron $\mathcal{T}$ in the full integral is then given by

$$g_{\mathcal{T}} \operatorname{tr}\big((Dw)_{\mathcal{T}}\big) \operatorname{vol}(\mathcal{T}) = g_{\mathcal{T}} \operatorname{tr}\big(WQ^{-1}\big) \frac{1}{6} \left|\det Q\right|. \tag{34}$$

A.2.5. *Computation of $\boldsymbol{j}_{\boldsymbol{q},\boldsymbol{\theta}} = \boldsymbol{\partial}_{\boldsymbol{w}}(\boldsymbol{j}_{\boldsymbol{q},\boldsymbol{\theta}}^{\top}\,\boldsymbol{w})$.* From equation (34), we obtain the derivatives

$$\partial_{w_0}\big(g_{\mathcal{T}} \operatorname{tr}\big(WQ^{-1}\big) \operatorname{vol}(\mathcal{T})\big) = -g_{\mathcal{T}} \operatorname{vol}(\mathcal{T}) \left(\mathbb{1}_3^{\top} Q^{-1}\right)^{\top}$$

and

$$\partial_{w_i}\big(g_{\mathcal{T}} \operatorname{tr}\big(WQ^{-1}\big) \operatorname{vol}(\mathcal{T})\big) = g_{\mathcal{T}} \operatorname{vol}(\mathcal{T}) \left((Q^{-1})_{i*}\right)^{\top} \quad \text{for } i = 1, 2, 3.$$

A.2.6. *Computation of $(\boldsymbol{\partial}_{\boldsymbol{q}}\boldsymbol{j}_{\boldsymbol{q},\boldsymbol{\theta}})^{\top}\boldsymbol{w} = \boldsymbol{\partial}_{\boldsymbol{q}}(\boldsymbol{j}_{\boldsymbol{q},\boldsymbol{\theta}}^{\top}\,\boldsymbol{w})$.* Again from (34), note that $g_{\mathcal{T}}$ is independent of q, so the derivatives from one tetrahedron are given by

$$\partial_{q_i}\big(g_{\mathcal{T}} \operatorname{tr}\big(WQ^{-1}\big) \operatorname{vol}(\mathcal{T})\big)$$
$$= g_{\mathcal{T}} \operatorname{vol}(\mathcal{T})\, \partial_{q_i}\big(\operatorname{tr}\big(WQ^{-1}\big)\big) + g_{\mathcal{T}} \operatorname{tr}\big(WQ^{-1}\big)\, \partial_{q_i}(\operatorname{vol}(\mathcal{T})) \quad \text{for } i = 0, \ldots, 3,$$

where

$$\partial_{q_0}\big(\operatorname{tr}\big(WQ^{-1}\big)\big) = \left(\mathbb{1}_3^{\top} Q^{-1} W Q^{-1}\right)^{\top}$$

and

$$\partial_{q_i}\big(\operatorname{tr}\big(WQ^{-1}\big)\big) = \left(-(Q^{-1}WQ^{-1})_{i*}\right)^{\top} \quad \text{for } i = 1, 2, 3.$$

References

[1] S. Adaszewski, J. Dukart, F. Kherif, R. Frackowiak, B. Draganski, A. D. N. Initiative, et al., *How early can we predict alzheimer's disease using computational anatomy?*, Neurobiology of aging, 34 (2013), pp. 2815–2826.

[2] M. B. Amar and A. Goriely, *Growth and instability in elastic tissues*, Journal of the Mechanics and Physics of Solids, 53 (2005), pp. 2284–2319.

[3] K. Amunts, C. Lepage, L. Borgeat, H. Mohlberg, T. Dickscheid, M.-É. Rousseau, S. Bludau, P.-L. Bazin, L. B. Lewis, A.-M. Oros-Peusquens, et al., *Bigbrain: an ultrahigh-resolution 3d human brain model*, Science, 340 (2013), pp. 1472–1475.

[4] N. Aronszajn, *Theory of reproducing kernels*, Transactions of the American mathematical society, 68 (1950), pp. 337–404.

[5] E. H. Aylward, B. Sparks, K. Field, V. Yallapragada, B. Shpritz, A. Rosenblatt, J. Brandt, L. Gourley, K. Liang, H. Zhou, et al., *Onset and rate of striatal atrophy in preclinical huntington disease*, Neurology, 63 (2004), pp. 66–72.

[6] M. F. Beg, M. I. Miller, A. Trouvé, and L. Younes, *Computing large deformation metric mappings via geodesic flows of diffeomorphisms*, International journal of computer vision, 61 (2005), pp. 139–157.

[7] H. Braak and E. Braak, *Neuropathological stageing of alzheimer-related changes*, Acta neuropathologica, 82 (1991), pp. 239–259.

[8] H. Braak and E. Braak, *Staging of alzheimer's disease-related neurofibrillary changes*, Neurobiology of aging, 16 (1995), pp. 271–278.

[9] A. Bressan and M. Lewicka, *A Model of Controlled Growth*, Archive for Rational Mechanics and Analysis, 227 (2018), pp. 1223–1266.

[10] B. Charlier, N. Charon, and A. Trouvé, *The fshape framework for the variability analysis of functional shapes*, J. Foundations of Comput. Math, 17 (2017), pp. 287–357.

[11] N. Charon and A. Trouvé, *The varifold representation of non-oriented shapes for diffeomorphic registration*, SIAM journal of Imaging Science, 6 (2013), pp. 2547–2580.

[12] H. Damasio, *Human brain anatomy in computerized images.*, Oxford university press, 1995.

[13] A. DiCarlo and S. Quiligotti, *Growth and balance*, Mechanics Research Communications, 29 (2002), pp. 449–456.

[14] J. Dompierre, P. Labbé, M. Vallet, and R. Camarero, *How to Subdivide Pyramids, Prisms, and Hexahedra into Tetrahedra*, in Proceedings of the 8th International Meshing Roundtable, 1999, pp. 195–204.

[15] S. Durrleman, X. Pennec, A. Trouvé, J. Braga, G. Gerig, and N. Ayache, *Toward a comprehensive framework for the spatiotemporal statistical analysis of longitudinal shape data*, International Journal of Computer Vision, 103 (2013), pp. 22–59.

[16] G. Gerig, B. Davis, P. Lorenzen, S. Xu, M. Jomier, J. Piven, and S. Joshi, *Computational anatomy to assess longitudinal trajectory of brain growth*, in Third International Symposium on 3D Data Processing, Visualization, and Transmission (3DPVT'06), IEEE, 2006, pp. 1041–1047.

[17] A. Goriely, *The mathematics and mechanics of biological growth*, vol. 45, Springer, 2017.

[18] D.-N. Hsieh, S. Arguillère, N. Charon, M. I. Miller, and L. Younes, *A model for elastic evolution on foliated shapes*, in Information Processing in Medical Imaging, A. C. S. Chung, J. C. Gee, P. A. Yushkevich, and S. Bao, eds., Springer International Publishing, 2019, pp. 644–655.

[19] X. Hua, B. Gutman, C. P. Boyle, P. Rajagopalan, A. D. Leow, I. Yanovsky, A. R. Kumar, A. W. Toga, C. R. Jack Jr, N. Schuff, et al., *Accurate measurement of brain changes in longitudinal mri scans using tensor-based morphometry*, Neuroimage, 57 (2011), pp. 5–14.

[20] D. C. Lin, C. P. McGowan, K. P. Blum, and L. H. Ting, *Yank: the time derivative of force is an important biomechanical variable in sensorimotor systems*, Journal of Experimental Biology, 222 (2019).

[21] O. Lindberg, M. Walterfang, J. C. Looi, N. Malykhin, P. Östberg, B. Zandbelt, M. Styner, B. Paniagua, D. Velakoulis, E. Örndahl, et al., *Hippocampal shape analysis in alzheimer's disease and frontotemporal lobar degeneration subtypes*, Journal of Alzheimer's Disease, 30 (2012), pp. 355–365.

[22] V. A. Lubarda and A. Hoger, *On the mechanics of solids with a growing mass*, International journal of solids and structures, 39 (2002), pp. 4627–4664.

[23] J. Ma, M. I. Miller, and L. Younes, *A bayesian generative model for surface template estimation*, International journal of biomedical imaging, 2010 (2010).

[24] J. E. Marsden and T. J. Hughes, *Mathematical foundations of elasticity*, Courier Corporation, 1994.

[25] M. I. Miller, L. Younes, J. T. Ratnanather, T. Brown, H. Trinh, D. S. Lee, D. Tward, P. B. Mahon, S. Mori, M. Albert, et al., *Amygdalar atrophy in symptomatic alzheimer's disease based on diffeomorphometry: the biocard cohort*, Neurobiology of aging, 36 (2015), pp. S3–S10.

[26] A. Qiu, M. Albert, L. Younes, and M. I. Miller, *Time sequence diffeomorphic metric mapping and parallel transport track time-dependent shape changes*, NeuroImage, 45 (2009), pp. S51 – S60.

[27] J. T. Ratnanather, S. Arguillère, K. S. Kutten, P. Hubka, A. Kral, and L. Younes, *3d normal coordinate systems for cortical areas*, arXiv preprint arXiv:1806.11169, (2018).

[28] L. Simon, *Lecture notes on geometric measure theory*, Australian national university, 1983.

[29] N. Singh, J. Hinkle, S. Joshi, and P. T. Fletcher, *A hierarchical geodesic model for diffeomorphic longitudinal shape analysis*, in International Conference on Information Processing in Medical Imaging, Springer, 2013, pp. 560–571.

[30] T. Tallinen, J. Y. Chung, F. Rousseau, N. Girard, J. Lefèvre, and L. Mahadevan, *On the growth and form of cortical convolutions*, Nature Physics, 12 (2016), p. 588.

[31] X. Tang, C. A. Ross, H. Johnson, J. S. Paulsen, L. Younes, R. L. Albin, J. T. Ratnanather, and M. I. Miller, *Regional subcortical shape analysis in premanifest huntington's disease*, Human Brain Mapping, 40 (2019), pp. 1419–1433.

[32] J. P. Ward and J. King, *Mathematical modelling of avascular-tumour growth*, Mathematical Medicine and Biology: A Journal of the IMA, 14 (1997), pp. 39–69.

[33] L. Younes, *Shapes and diffeomorphisms*, vol. 171, Springer Science & Business Media, 2010.

[34] L. Younes, *Hybrid riemannian metrics for diffeomorphic shape registration*, Annals of Mathematical Sciences and Applications, 3 (2018), pp. 189–210.

[35] L. Younes, M. Albert, A. Moghekar, A. Soldan, C. Pettigrew, and M. I. Miller, *Identifying changepoints in biomarkers during the preclinical phase of alzheimer's disease*, Frontiers in Aging Neuroscience, 11 (2019), p. 74.

[36] L. Younes, K. S. Kutten, and J. T. Ratnanather, *Normal and equivolumetric coordinate systems for cortical areas*, arXiv preprint arXiv:1911.07999, (2019).

[37] L. Younes, J. T. Ratnanather, T. Brown, E. Aylward, P. Nopoulos, H. Johnson, V. A. Magnotta, J. S. Paulsen, R. L. Margolis, R. L. Albin, et al., *Regionally selective atrophy of subcortical structures in prodromal hd as revealed by statistical shape analysis*, Human brain mapping, 35 (2014), pp. 792–809.